Politecnico di Torino

Internal resonance of structure subjected to large deformations

Pietro Bernuzzi

Supervisors
Prof. Dario Anastasio, Supervisor
Prof. Stefano Marchesiello, Co-Supervisor

Politecnico di Torino
July 23, 2025

Contents

1. Introduction

1.1 Linearization and linear systems

As it normally happens, structural engineering studies are portrayed under ideal conditions: isotropy, constant section properties and other hypothesis, that simplifies the utilised methodologies. Such ideal conditions enable the researcher to get a manageable data analysis and to focus on the overall mechanical behaviour of the system which is under study. In particular, in structural dynamics engineering studies, small displacements or small deformations relative to the static equilibrium position are systematically used. Both small displacement and small deformations allow to use an effective methodology: the linearization. The linearization is one of the most used methods in dynamic analysis. It allows to obtain the solution of complex problems with low computational effort, foreseeing the dynamic behaviour of a mechanical system.

To clarify how the linearization works is proposed below an example, contained in the book of Benson H. Tongue "Principle of Vibrations" which consider a rotational single degree of freedom, a pendulum, from which its equation of motion, the mathematical model which describes how such system moves, is calculated.

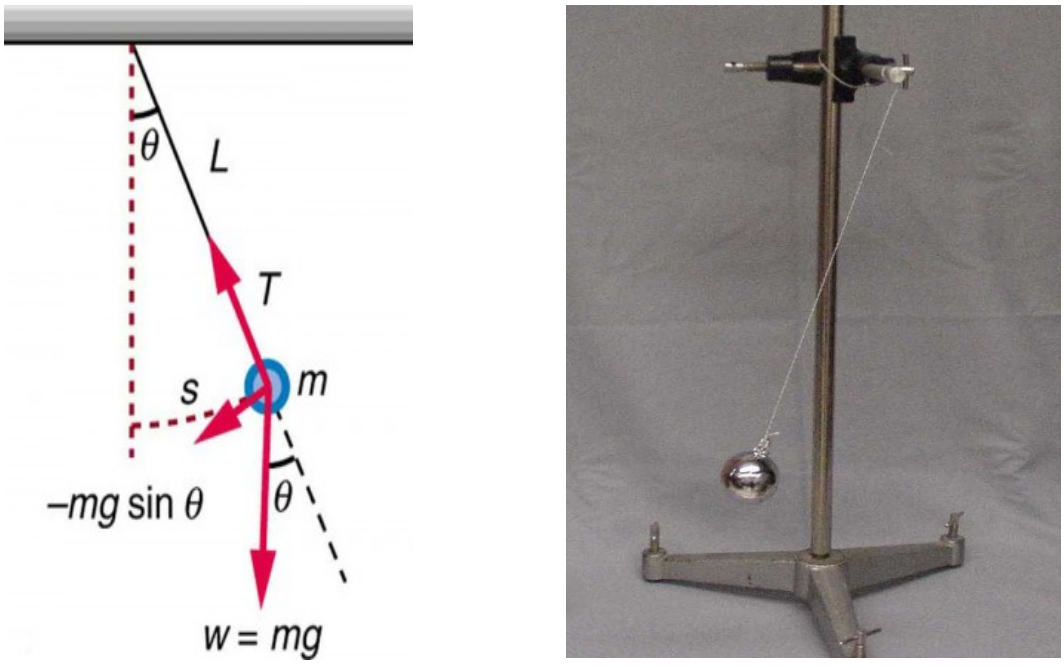

Figure 1.1: Pendulum representation and pendulum picture.

$$ml^2\ddot{\theta} + mglsin(\theta) = 0 \qquad (1.1)$$

The pendulum equation of motion is nonlinear because it needs higher than first power of the dependent variable θ and its derivative. After expanding sin(θ), the equation can be solved by applying the linearization method, which consists in neglecting all terms that do not depend linearly on θ or its derivatives—that is, terms where θ or its derivatives appear with powers higher than one. Below it is showed the expansion of the sin function in the nonlinear form (1.2) and the linearized equation of motion (1.3). The omitted data result vanishingly small when the variable θ is small.

$$sin(\theta) = \theta - \frac{1}{3}\theta^3 + \cdots \quad (1.2)$$

$$\ddot{\theta} + \frac{g}{l}\theta = 0 \quad (1.3)$$

In the analysis of the mathematical model of the pendulum dynamics, the linearization simplifies the equation of motion and assuming a small-angle approximation, valid when the angular displacement remains below 5° from the equilibrium position, the resulting oscillation amplitudes can be considered physically realistic.. It is noteworthy the power of the tool that makes systems linear, indeed allow the equation to become an ordinary differential, so simplifying the resolution of mathematical model.

Moreover, the advantages of linearization are those of making a system to be modelled as linear. The key characteristics of a linear system are:

- Linearity: The system must satisfy the principle of superposition, meaning that if the input is a linear combination of two signals, the output is also the linear combination of the corresponding individual outputs.
- Homogeneity: This is a specific aspect of linearity. If the input is scaled by a factor, the output is also scaled by the same factor.
- Additivity: The response of the system to the sum of two inputs is equal to the sum of the responses to each input individually.
- Time Invariance: The system's behaviour does not change with time. If the input signal is delayed or advanced in time, the output is similarly delayed or advanced without any change in shape.

These characteristics are widely used in dynamics because they allow for a generalized and simplified analysis of complex systems. Based on these properties, many solution methods have been developed. In effect, linearization results in systems that are predictable, scalable, and time-invariant, which greatly simplifies the mathematical calculus. Acknowledging that linearization simplifies the analysis, it is though necessary to formulate a mathematical model that simulate how real systems behave with the aim of being aware of the differences between ideal and real-world dynamics.

Dynamical system can be modelled as discrete (single or multi degree) or continuous. A degree of freedom (DOF) in mechanics and engineering refers to the number of independent ways a system can move or the minimum number of independent variables needed to define its configuration or motion. The equation of motion of a single degree of freedom is retrieved thank to the Newton's second law, characterized by three different parameters:

- mass (m)
- stiffness (k)
- damping (c).

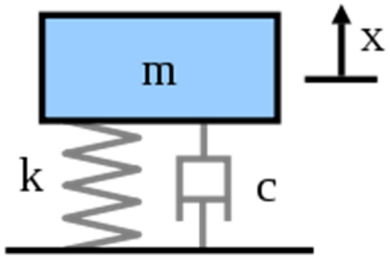

Figure 1.2: Single degree of freedom representation.

$$m\ddot{x} + c\dot{x} + kx = 0 \qquad (1.4)$$

The single degree of freedom is characterized by:

- one mode shape which is how the system moves or deform,
- a natural frequency at which the system oscillates in the absence of any driving force, that is calculated as the square root of the ratio of stiffness and mass.

A n-degree of freedom is a system characterized by n independent variable and thus n natural frequencies. It has n equations of motion, which are ordinary differential equations, and are collected in matrices.

For what concerns continuous systems, they consist of an infinite number of particles, hence need an infinite number of ordinary differential equations to describe their motion. However, because the distance between two adjacent particles is infinitesimal and displacements must be continuous, the motion of a continuous system is described by a finite number of displacement variables. Dynamics of continuous systems can be expressed in terms of partial differential equations with appropriate boundary conditions.

Moreover, continuous systems are categorized in terms of geometries and loading conditions, each of them is described by a precise partial differential equation. They are grouped in six categories: cables, bars, beams, membranes, plates and shells.

The beam element is a system in which one dimension is larger than the others. It often has a straight axis and a prismatic section. Two formulations are famous to describe the dynamic behaviour of a beam:

- Euler-Bernoulli formulation
- Timoshenko formulation.

The Euler Bernoulli beam is the simplest approach to describe the flexural behaviour of a beam, it considers just bending deformation and translational inertia. The Timoshenko beam considers further the rotational inertia of the cross section and the shear deformation.

The mathematical model described in the next chapter, is constituted of Euler-Bernoulli beam elements. The partial differential equation of an infinitesimal section is characterized by two terms coming from the vertical translation and moments equilibrium. It is reported below:

$$\frac{\partial^2}{\partial x^2}\left(EI\frac{\partial^2 v}{\partial x^2}\right)+\mu\frac{\partial^2 v}{\partial t^2}=f(x,t) \qquad (1.5)$$

Where:

- $v(x,t)$: is the transverse displacement of the beam at position x and time t,
- E: is the Young's modulus (material stiffness),
- $I(x)$: is the second moment of area (which may vary along the beam),
- EI: represents the flexural rigidity of the beam (resistance to bending),
- μ : is the mass per unit length,
- $f(x,t)$: is the external distributed load (force per unit length) as a function of space and time

In the particular case in which the applied force is null and the section is constant throughout the beam, the equation is simplified as:

$$EI\left(\frac{\partial^4 v}{\partial x^4}\right)+\mu\frac{\partial^2 v}{\partial t^2}=0 \qquad (1.6)$$

The equation is then solved using the separation of variable theorem: the variable v can be written as the product of one time-depending variable and one spatial-depending variable. The derivative of the time-dependent variable is simply the function multiplied to the negative square of the frequency. A time-dependent quantity equals a spatially varying quantity if only they are both equal to a constant:

$$v(x)''''-\beta^4 v(x)=0 \qquad (1.7)$$

Where:

$$\beta = \sqrt[4]{\frac{\rho A w^2}{EI}}$$

The solution of the equation just showed is the so called *eigen-function* which is composed by four parameters computed through the boundary condition:

$$v(x) = \mathrm{a}\sin(\beta x) + \mathrm{b}\cos(\beta x) + \mathrm{c}\sinh(\beta x) + \mathrm{d}\cosh(\beta x) \qquad (1.8)$$

1.2 Nonlinear systems

In dynamics, engineers must predict how systems move and respond to inputs, with the goal of replicating real behaviour as closely as possible. This objective does not always align with the assumptions of linear modelling. Linearization alone may not be sufficient, and understanding nonlinear behaviour is crucial to accurately simulate real-world dynamics.

Nonlinear systems are those for which the principle of superposition does not hold. The sources of nonlinearities can be material or constitutive, geometric, inertia, body forces, or friction. The constitutive nonlinearity occurs when the stress are nonlinear functions of the strains, the geometric nonlinearity is associated with large deformations in solid resulting in nonlinear strain-displacement relation. The inertia nonlinearity may be caused by the presence of concentrated or distributed masses. The nonlinear body forces are essentially magnetic and electric forces. The friction nonlinearity occurs because the friction force is a nonlinear function of the displacement and velocity.
In particular, geometric nonlinearities are studied in this thesis. When the lateral deflection of a beam is large, the axial force plays a significant role in carrying transverse loads, and geometric nonlinearities couple the equations governing the extension and bending vibrations. Moreover, for an isotropic beam, linear formulation shows that the vibrations in the two principal planes are independent of each other, and hence a forced motion in one principal plane always remains in that plane. But, when the vibration amplitude is large, the motion may become nonlinear due to geometric nonlinear coupling between bending in two principal planes. [1]

Once the causes are explained, the symptoms or consequences of nonlinear behaviors are illustrated. To clearly present the nonlinear symptoms, a nonlinear single degree of freedom system is considered. It is studied the undamped harmonic response of the SDOF system.

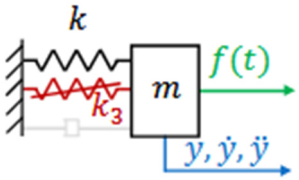

Figure 1.5: Nonlinear single degree of freedom with cubic stiffness

$$m\ddot{y} + ky + k_3 y^3 = Fe^{i\Omega t} \quad (1.9)$$

The equation of motion contains cubic stiffness which makes the system nonlinear. When subjected to a harmonic input with a frequency Ω, the presence of the cubic stiffness generally generates harmonic contributions of the kind 3Ω, 5Ω, …
Such phenomenon is called harmonic distortion. Experimentally, it appears in the frequency spectrum as peaks not only at the excitation frequency but also at higher harmonics. Harmonic distortion can significantly affect a system's dynamic behaviour. For instance, in a multi-degree-of-freedom (MDOF) system, a mode that is not directly excited can be activated by a harmonic of another mode. Similarly, closely spaced modes can exchange energy through nonlinear interactions. When natural frequencies are commensurable or nearly commensurable, internal resonance phenomena may occur, which is a special case of modal interactions. Internal resonance makes the system to exchange energy between the internally coupled modes. The extent of the interaction and its conditions depend on the linear natural frequencies and the nonlinearities of the system.

1.3 Vibration Energy Harvesting and the Role of Piezoelectric Materials

Vibration control has long been a key focus in engineering, with passive strategies such as vibration absorption and isolation commonly employed to mitigate unwanted mechanical oscillations. Traditionally, methods like nonlinear energy sinks (NES) are used to dissipate vibrational energy and protect structures. However, rather than merely suppressing vibrations, an alternative and increasingly attractive approach involves harnessing this energy. This has given rise to the concept of vibration energy harvesting (VEH) - a clean and sustainable method for converting ambient mechanical vibrations into usable electrical energy.

VEH technology is particularly well-suited for powering small, low-consumption electronic devices such as wireless sensors and embedded systems. By reducing or eliminating the need for batteries, VEH contributes to improved energy efficiency and environmental sustainability. However, the electrical power harvested from environmental vibrations is typically limited, necessitating efficient transduction mechanisms and design strategies.

The most common VEH systems are based on linear resonance principles, where the harvester is tuned to match a dominant ambient vibration frequency. When properly tuned, these systems operate efficiently, but they suffer from a critical limitation: a narrow operational bandwidth. This means they are only effective when the excitation frequency closely aligns with their resonant frequency. Any deviation can result in a significant drop in energy harvesting performance.

To overcome this limitation, recent research has explored broadband energy harvesting techniques. These methods are designed to capture vibrational energy over a wider frequency range, improving adaptability to varying environmental conditions. One promising approach involves the use of internal resonance, wherein nonlinear interactions between different modes of vibration enable energy transfer across frequencies. Although this introduces complexity into the system's frequency response, it also facilitates nonlinear dynamic behavior that can substantially broaden the effective bandwidth of the harvester.

A key enabler of VEH systems—particularly those incorporating nonlinear dynamics—is the use of piezoelectric materials. These materials generate an electric charge when subjected to mechanical stress, a property known as the piezoelectric effect, first discovered by Pierre and Jacques Curie in 1880. Remarkably, the reverse effect also exists: applying an electric field can induce a mechanical deformation in the material.

Due to these unique electromechanical coupling properties, piezoelectric materials are employed in a wide range of technologies, including sensors, actuators, ultrasonic transducers, and medical imaging devices. In the context of VEH, their ability to directly convert mechanical vibrations into electrical energy makes them particularly valuable.

1.4 Thesis structure

The structure of the thesis is as follows:

- Chapter 2 explores nonlinear system behavior in detail, providing key theoretical tools and examples needed to analyze the system, beyond the linear regime.
- Chapter 3 presents the design and modeling of the system, including the construction of a finite element model.
- Chapters 4–6 detail the experimental procedures, data acquisition techniques, and validation strategies employed to confirm theoretical predictions.
- The final chapter offers conclusions and suggests future directions for improving VEH designs through advanced modeling, multi-physics simulations, and adaptive control.

This research aims to bridge the gap between idealized models and practical engineering applications, showing how nonlinear effects—often considered a complication—can instead be leveraged to improve performance in energy harvesting systems.

2. System design

The mechanical system that will be utilized in the research is a structure of which one of the characteristics is the response with internal resonance caused by solicitation. Normally, a linear energy harvester collects ambient vibration energy if the input frequency matches its resonance region. Hence, the bandwidth of the effective operating frequency is usually limited to a specific range. If the ambient vibration frequency slightly deviates from the resonant frequency of the energy harvesting device, the resulting power output of harvesters would be reduced drastically. [2] To overcome such problems, the nonlinear studied vibration harvester is designed to exhibit an internal resonance which enlarge the operating bandwidth, increasing the energy conversion.
The solicitation at which the structure is subjected is vertical and with a frequency of approximately 20 Hz, exciting exactly the second natural frequency. It will be described in detail the structure that will be utilized for the research. From the image shown below, the design of such object could be obtained, which:

- Is rectangular
- Is constituted of aluminum with a density of 2700 kg/m^3
- Is located on an electrodynamic shaker used to test the structure
- Is 165 mm × 230 mm × 20.5 mm, with a thickness of 0.65 mm.

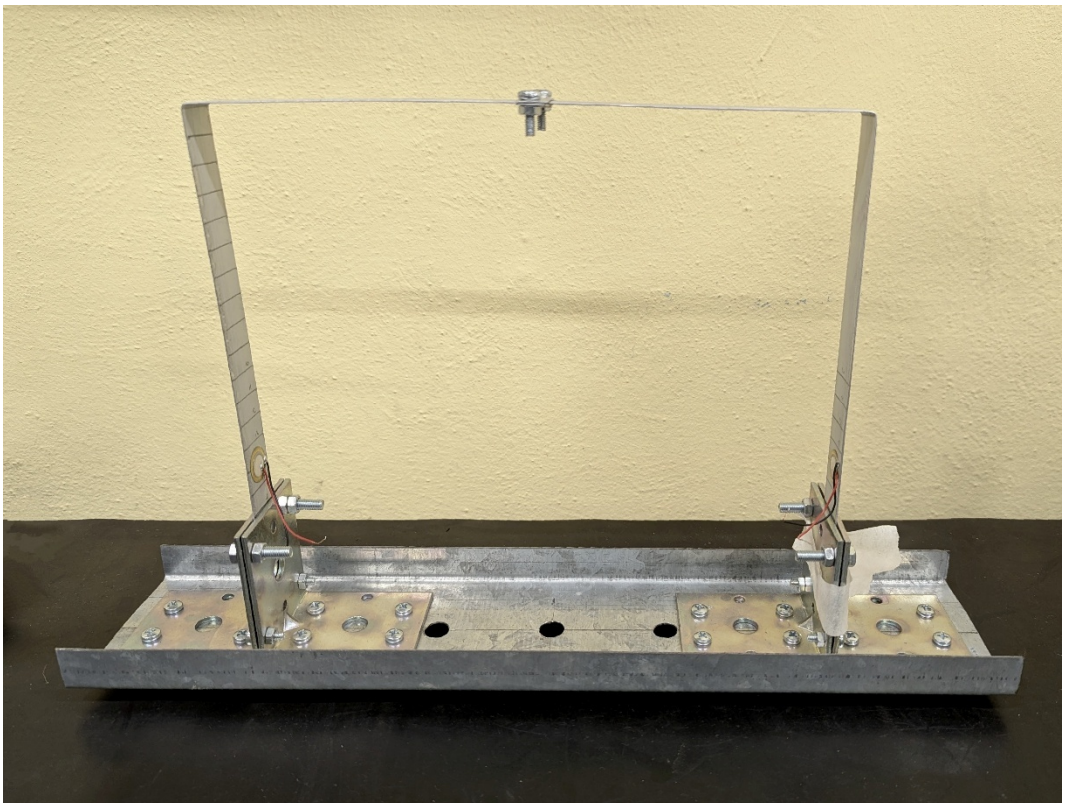

Figure 2.1: Picture of the portal frame

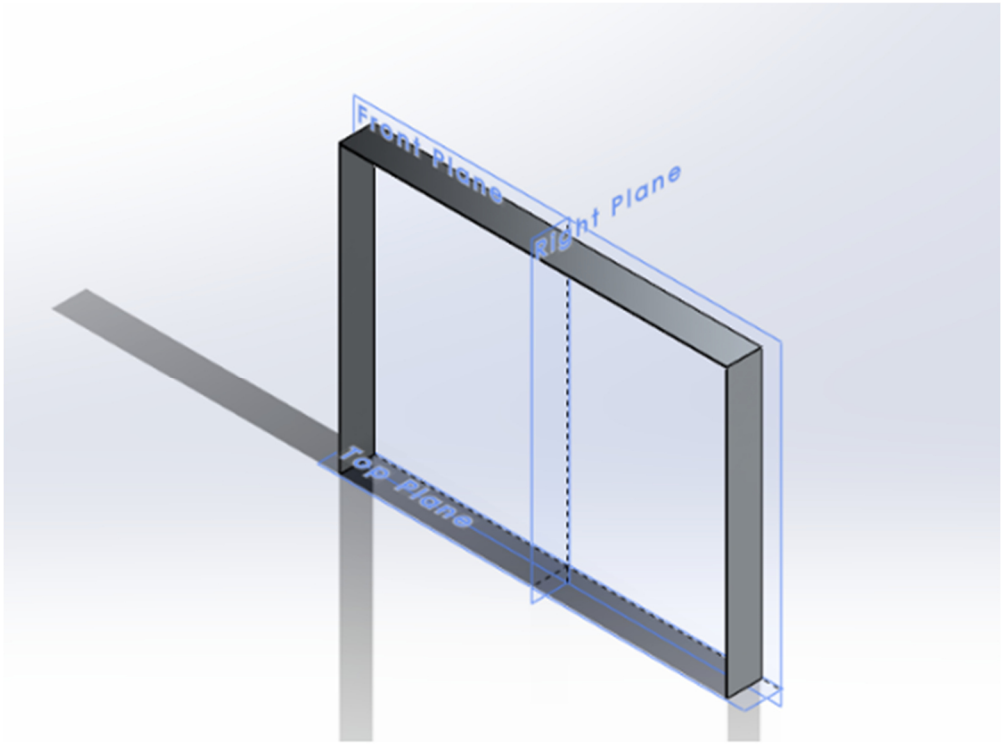

Figure 2.2: System without accelerometers

The structure is instrumented with two accelerometers located in the middle of the horizontal beam, as seen in Figure 2.3. The two sensors measure accelerations in vertical and horizontal directions.

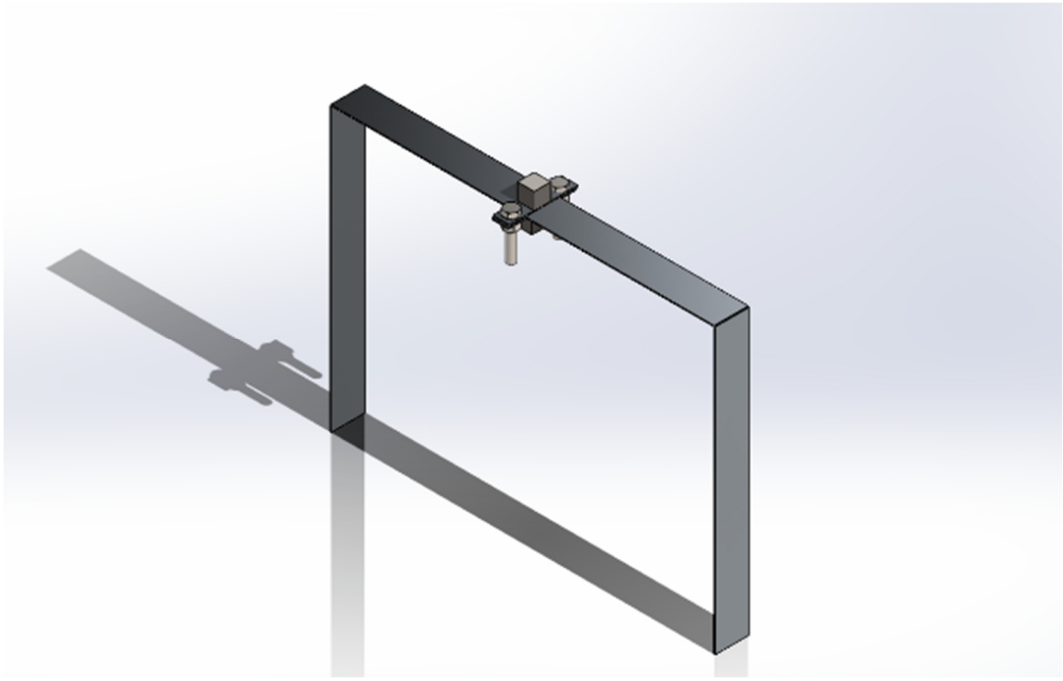

Figure 2.3: System with accelerometers

The finite element model of the VEH is designed using two different software: Solidworks and Ansys APDL. The first software, Solidworks, permits to reproduce the portal frame. It is designed also the portal with two accelerometers attached.

As for Ansys APDL, the following elements are adopted:

- BEAM188 is the element used to represent the structure, it is a 3D element suitable for analysing slender to moderately stubby/thick beam structures. The element is based on Timoshenko beam theory which includes shear-deformation effects.
- MASS184 is the element used to represent a rigid connection.
- MASS21 is the element used for representing the accelerometers because is a point element.

The geometry is then divided into small segments on which elements are built. Such a step is particularly important because according to the number of segments, and hence elements, the result of the simulation will be precise or inaccurate. It is also shown a picture that represents and lists the nodes of the model. A specific set of nodes will be chosen and for such nodes the displacement will be shown.

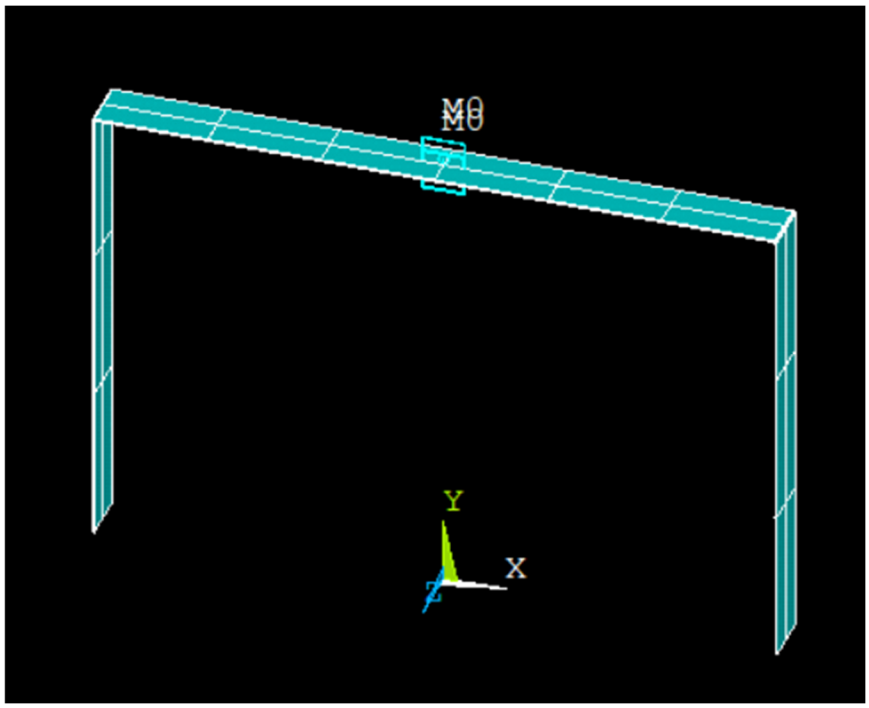

Figure 2.4: Definition of the elements of the frame

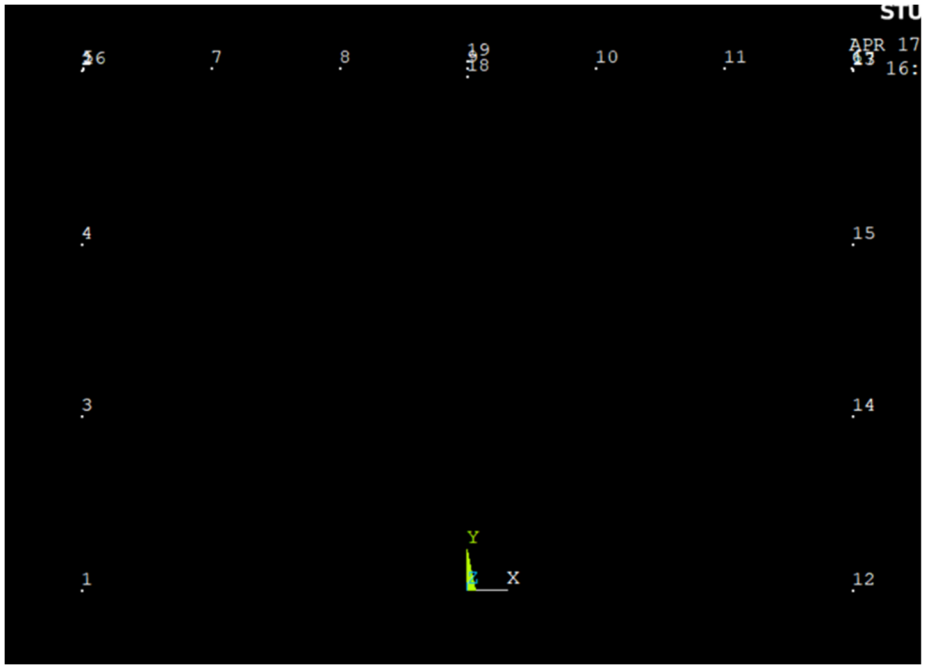

Figure 2.5: Geometry of the frame with nodes numbering (16 elements)

2.1 Theoretical linear model

The structure has been modelled through the Euler-Bernoulli beam formulation, which is a simplification of the linear theory of elasticity and is used to compute the load-carrying and deflection characteristics of beams. In contrast to the Timoshenko formulation, the Euler-Bernoulli formulation neglects the contributions of the shear deformation and of the rotary inertia. Neglecting the shear contribution is a correct approximation when the beam does not wiggle too much or in the low natural frequencies. For what concerns the rotary inertia approximation, it is a reasonable assumption when the length of the beam is 10 times greater than the height. Both requirements are respected since only the first two natural frequencies analysed along the experiment and since the U-shaped frame beams have a length way greater than the height.

The U-shaped frame has been built using three Euler-Bernoulli beams attached one to the other (the small fillet are neglected in the analytical model) and it has two fixed constraints that block the displacements in every direction and every rotation. The reason why will be highlighted in the next chapter, though it's important to model the accelerometers: they are easily taken into account by imposing a mass in the middle point of the horizontal beam.

Four boundary conditions are needed to properly solve a Euler-Bernoulli equation of motion, four are the parameters that compose the eigenfunction used to solve the equation. Then, the resolution of the linear analytical model of the frame implies 16 boundaries conditions which are collected below:

$$v_1(0,t) = 0 \tag{2.1}$$
$$v_1'(0,t) = 0 \tag{2.2}$$
$$v_4(L_4,t) = 0 \tag{2.3}$$
$$v_4'(L_4,t) = 0 \tag{2.4}$$
$$v_2(0,t) = 0 \tag{2.5}$$
$$v_1'(L_1,t) = v_2'(0,t) \tag{2.6}$$
$$E_b I_b v_1''(L_1,t) = E_b I_b v_2''(0,t) \tag{2.7}$$
$$v_2(L_2,t) = v_3(0,t) \tag{2.8}$$
$$v_2'(L_2,t) = v_3'(0,t) \tag{2.9}$$
$$E_b I_b v_2''(L_2,t) = E_b I_b v_3''(0,t) \tag{2.10}$$
$$E_b I_b v_2''(L_2,t) = m_t v_2(L_2,t) + E_b I_b v_3''(0,t) \tag{2.11}$$
$$v_3(L_3,t) = 0 \tag{2.12}$$
$$v_3'(L_3,t) = v_4'(0,t) \tag{2.13}$$
$$E_b I_b v_3''(L_3,t) = E_b I_b v_4''(0,t) \tag{2.14}$$
$$v_1(L_1,t) = -v_4(0,t) \tag{2.15}$$
$$E_b I_b v_1'''(L_1,t) + E_b I_b v_3''(0,t) = (\rho_b A_b (L_2 + L_3) + m_t)\ddot{v}_1(L_1,t) \tag{2.16}$$

The determinant of the matrix solving the system of equation is plotted in the figure below.

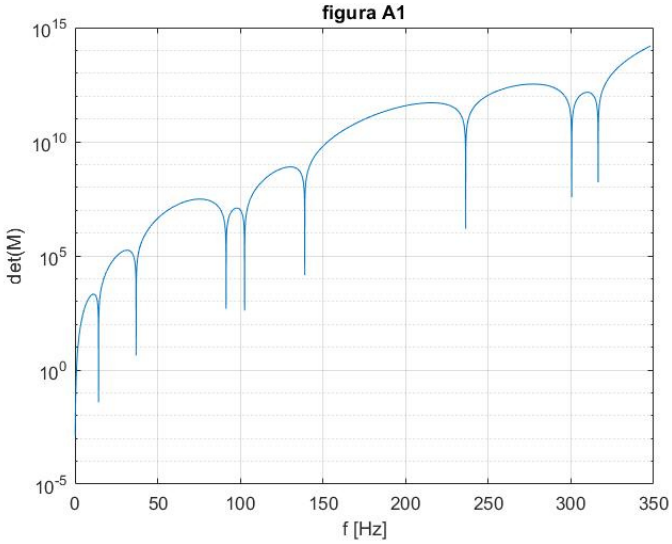

Figure 2.6: Representation of the determinant function of the eigenvalues matrix

The mode shapes related to the first two natural frequencies are plotted as well below.

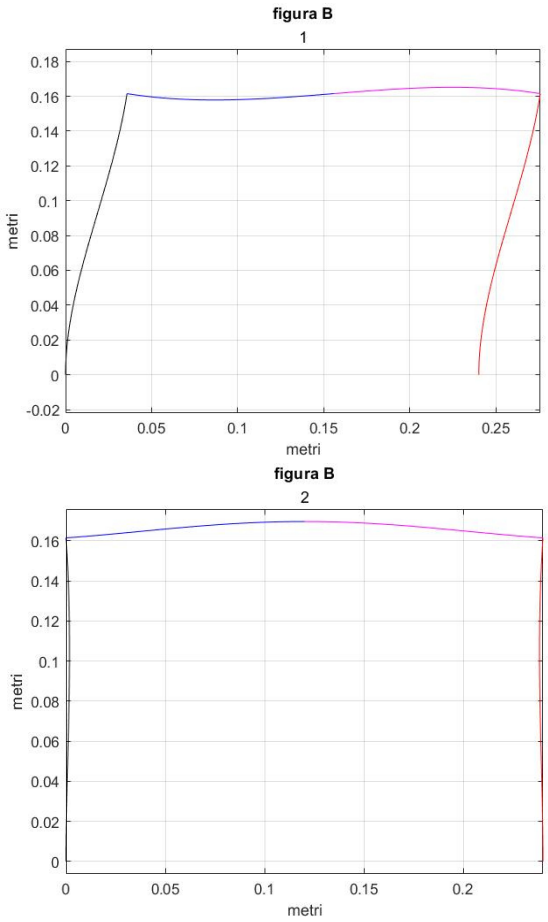

Figure 2.7: Picture (1) represents the first mode shape of the frame; Picture (2) represents the second mode shape

3. Preliminary test and model updating

The outcomes of the experimental measurement are the foundation of the digital twin development. Before proceeding to the analysis of the research, it is necessary to perform preliminary test on the object. Such preliminary tests are:

- Random vibration analysis: the illustrated structure is subjected to random vibrations to excite all the frequencies and detect the natural ones.

3.1 Quantification of the uncertainties

The experimental measurements have revealed that the dynamic response signal of the frame is influenced by the presence of the cables that link the accelerometers to the analog to digital converter. The procedure adopted for the accelerometers, which was to simplify them as mass points, could not be repeated for the cables because they are attached all along the structure, affecting the overall damping of the frame.

Even if it does not reflect the reality, the method chosen to model the cable is to add a mass to the mass points representing the accelerometers and to vary the model parameters, the length, the width or the thickness of the system, until the dynamic response of the designed frame is similar to the experimental measurements. The method is effective, but it requests several iterations to reach a precise result.
For the sake of simplicity, the procedure has been applied to the linear model which has been tuned in order to have similar natural frequencies with respect to the extrapolated from the measurements. Tuning the model to the experimental results means to vary the system properties in order to have outputs similar to the ones of the physical object with the same input. It helps to understand which properties of the system affect to a large scale the dynamic behaviour.

Table 2 contains a series of simulations or experimental tests where the natural frequencies of the first (W_1) and second (W_2) vibration modes of a structure are recorded, while varying some physical and geometrical parameters: material density, lengths (L_1, L_2), width (w), and thickness (s). All values are expressed in SI units.

Main Observations:

- Material Density

  The density ranges from 2650 to 2750 kg/m^3, which is typical for aluminum. An increase in density generally leads to a reduction in the natural frequencies.

- Lengths L_1 and L_2

  Minor dimensional variations were explored:

  - L_1 varies between approximately 0.156 m and 0.168 m
  - L_2 ranges from 0.115 m to 0.125 m

  Even small changes in length significantly affect the frequencies: an increase in length (especially L_1) tends to reduce natural frequencies due to the decrease in flexural stiffness.

- Width (w) and Thickness (s)

  The width ranges from 0.0185 m to 0.0205 m, while the thickness varies between 0.0005 m and 0.0007 m.

  - An increase in thickness results in a clear rise in natural frequencies, confirming the high sensitivity of flexural stiffness to thickness variation (since the second moment of area $I \propto s \cdot w^3$ or $w \cdot s^3$ depending on orientation).
  - The effect of width variation is less pronounced but still observable.

Frequency Response:

- The first mode frequency varies from approximately 11.78 Hz to 15.73 Hz.
- The second mode spans from 28.55 Hz to 42.86 Hz.
- The combined effect of geometric and mass variations leads to a maximum deviation of up to 35% for the second mode and around 25% for the first, highlighting the system's sensitivity.

This parametric analysis aims to assess the sensitivity of the system's dynamic behavior to changes in physical and geometrical parameters. These insights are fundamental during the model updating phase, helping to align numerical models with experimental data. They also support the evaluation of nonlinear structural effects, such as internal resonance, which may emerge under specific mass and geometry configurations.

Density $(\frac{kg}{m^3})$	**L1** (m)	**L2** (m)	**w** (m)	**s** (m)	$W_1(Hz)$	$W_2(Hz)$
2700	0.162	0.12	0.0195	0.0006	14.14	36.74
2750	0.162	0.12	0.0195	0.0006	14.01	36.40
2650	0.162	0.12	0.0195	0.0006	14.27	37.08
2700	0.168	0.12	0.0195	0.0006	13.38	36.33
2700	0. 156	0.12	0.0195	0.0006	14.96	37.14
2700	0.162	0.125	0.0195	0.0006	13.85	28.55
2700	0.162	0.115	0.0195	0.0006	14.43	39.48
2700	0.162	0.12	0.0205	0.0006	14.14	36.74
2700	0.162	0.12	0.0185	0.0006	14.14	36.74
2700	0.162	0.12	0.0195	0.0007	15.73	42.86
2700	0.162	0.12	0.0195	0.0005	11.78	30.61

Table 1: influence of the frame dimensions on the natural frequencies

As said before, after some necessary iterations the results related to the frame without sensors are showed below. According to the standard, the percentage error has an acceptable range of 0 to 5 % which is respected for both the natural frequencies.
To estimate the mass of the cables an iterative procedure has been portrayed, and the results are collected in the table.

Modes	Experimental data (Hz)	Calculated results (Hz)	Error (%)
1	15.5	15.16	2
2	42.5	43.9	3

Table 2: Natural frequencies of the portal frame without accelerometers

As for the system with accelerometers and cables, the results are collected in the following table.

Modes	Experimental data (Hz)	Calculated results (Hz)	Error (%)
1	9.7	9.95	3
2	19.7	19.69	0

Table 3: Natural frequencies of the portal frame with accelerometers

3.2 Preliminary test data

The portal frame is excited through vertical random vibrations using the electrodynamic shaker. The graph below presents all the responses of the base vertical acceleration with an amplitude of 1.7 m/s^2 during 60 seconds of measurement:

- The first graph represents the random acceleration to which the model is subjected
- The second graph represents the vertical acceleration of the accelerometer cleared by the vertical acceleration of the base of the frame
- The third graph represents horizontal acceleration.

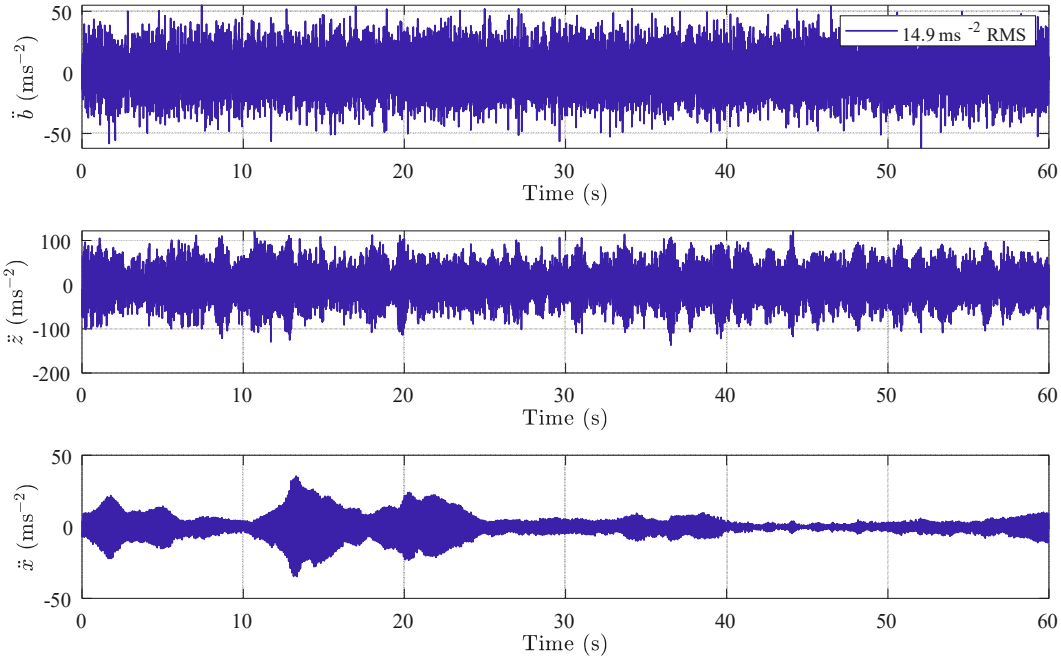

Figure 3.2.1: Diagrams of the base acceleration, of the relative vertical acceleration and of the horizontal acceleration

Collected data are postprocessed in the frequency domain in terms of transmissibility and coherence function. The transmissibility is defined as:

$$T(f) = \frac{\text{Output amplitude}}{\text{Input amplitude}}$$

The diagram stands for the vertical transmissibility, the ratio between the base acceleration and the vertical acceleration collected by the accelerometer.

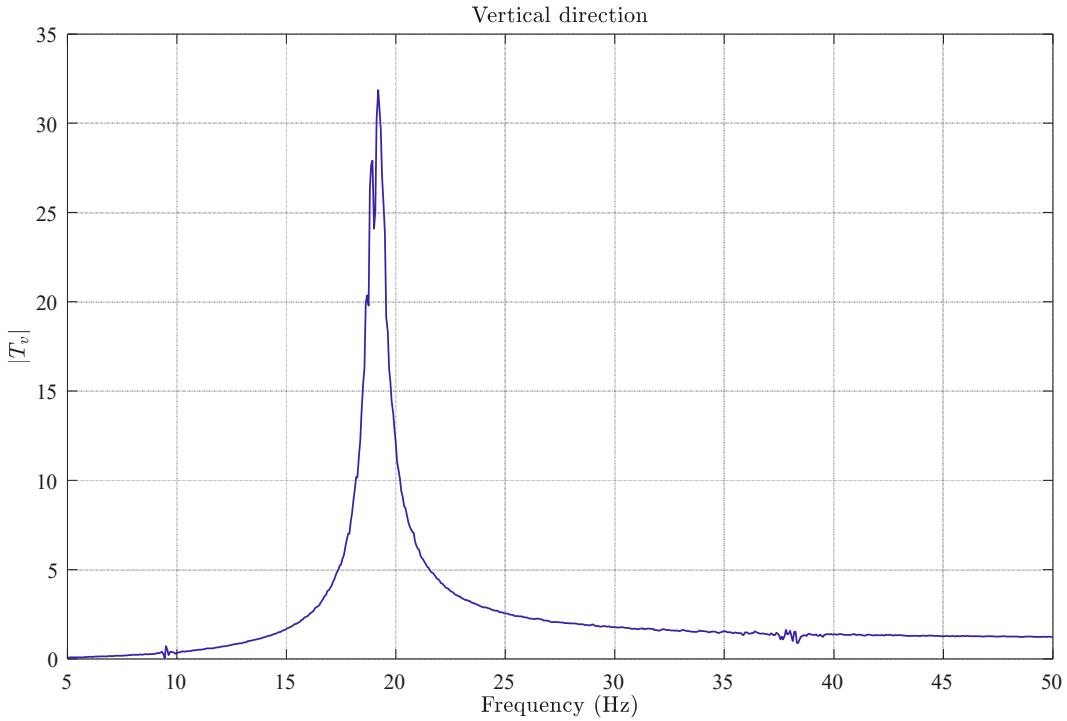

Figure 3.2.2: Graph of the vertical relative transmissibility

While the next diagram stands for horizontal transmissibility, the ratio between the base acceleration and the hizontal acceleration collected by the accelerometer.

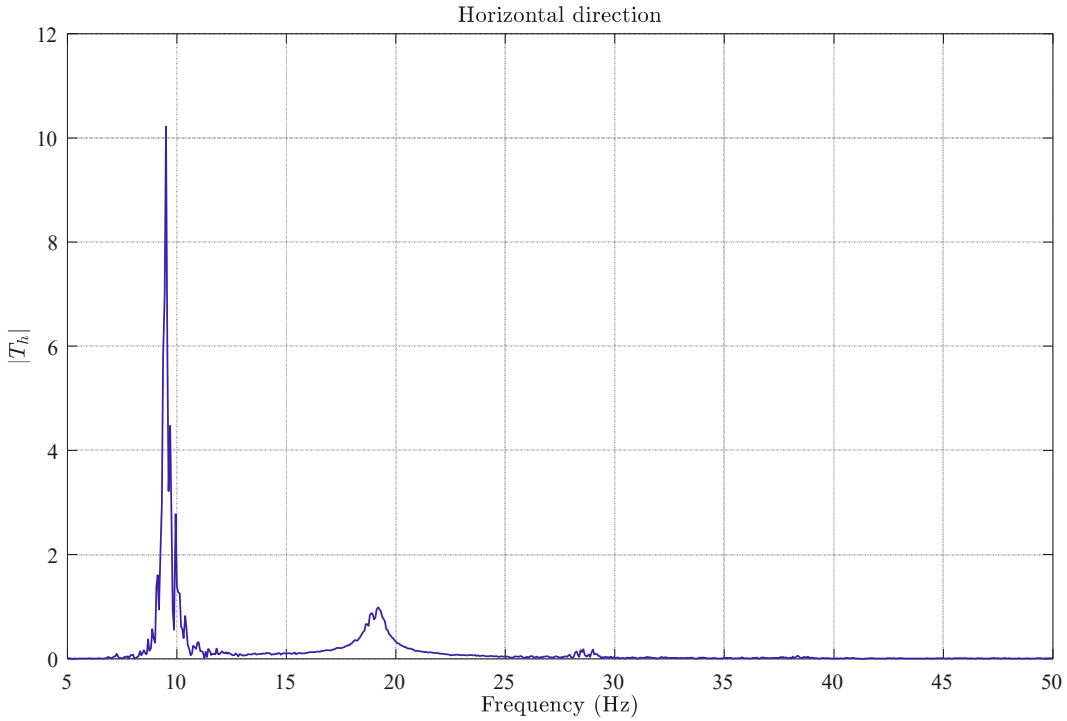

Figure 3.2.3: Graph of the horizontal transmissibility

The coherence function is an indicator that quantifies the degree of linear correlation between two signals at each frequency. It is particularly valuable in the context of systems characterized by input-output relationships.

The coherence function is mathematically defined as:

$$\gamma^2(\mathrm{f}) = \frac{|\ \mathrm{Gxy(f)}\ |}{2\mathrm{Gxx(f)} \cdot \mathrm{Gyy(f)}}$$

Where:

- $\mathrm{G}_{xy}(f)$: Cross-power spectral density between input x(t) and output y(t)
- $\mathrm{G}_{xx}(f)$: Auto-power spectral density of input
- $\mathrm{G}_{yy}\ (f)$: Auto-power spectral density of output
- $\gamma^2(f)$: Coherence, a function of frequency f

Coherence takes values in the range:

$$0 \leq \gamma^2(\mathrm{f}) \leq 1$$

A coherence value of 1 indicates a perfect linear relationship between input and output at the given frequency, whereas a value of 0 implies a complete lack of correlation, typically suggesting the presence of noise, nonlinearities, or other unmodeled dynamics. High coherence signifies that the system behaves in a predictable, linear manner, which is advantageous for system identification and transfer function modeling. Conversely, low coherence may be indicative of measurement noise, nonlinear system behavior, or unrelated external influences. In the graph presented below, the coherence associated with the vertical transmissibility tends to zero only in correspondence with the second natural frequency. This reduction in coherence is likely attributable to nonlinear dynamic behavior of the supporting frame structure.

i

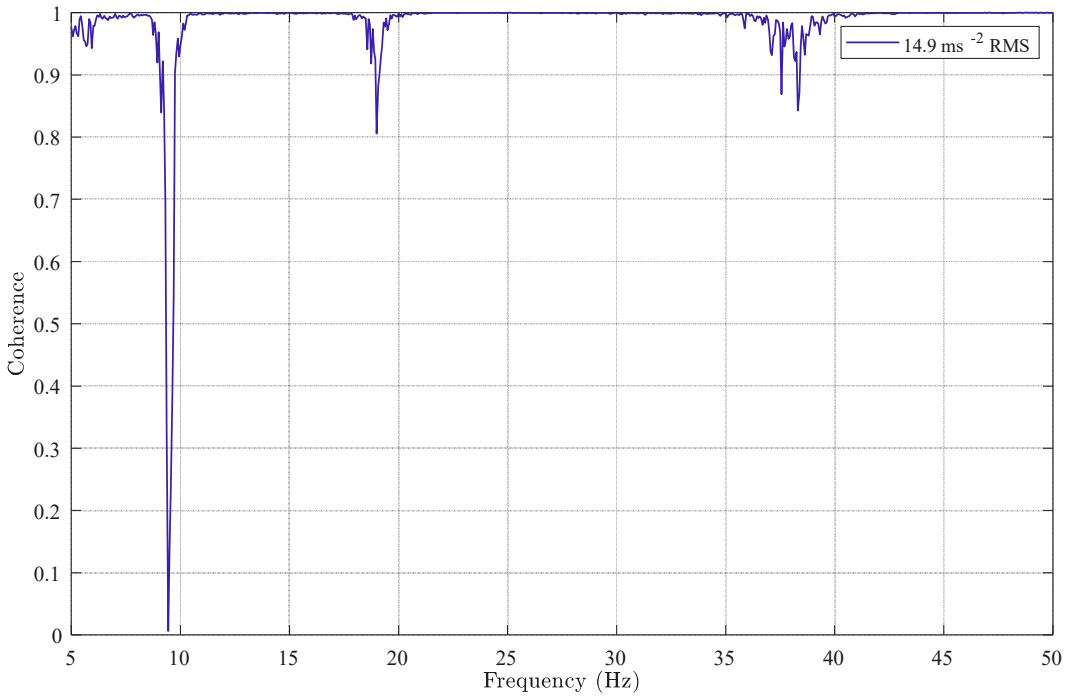

Figure 3.2.4: Coherence of the vertical relative transmissibility

In the case of the coherence of the horizontal transmissibility, the function coherence behaves as can be seen in the graph below.

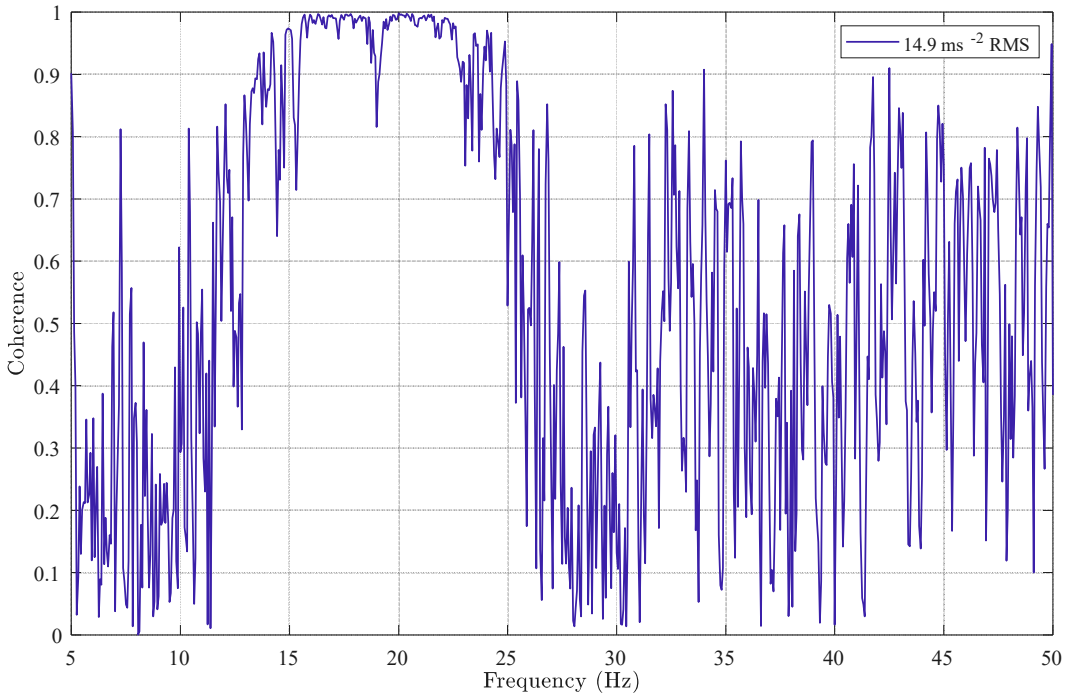

Figure 3.2.5: Coherence of the horizontal transmissibility

The diagram is different from the previous one since there is noise at the beginning, approximately to 0, and at the end of the measurement, approximately to 40 Hz,

while between 5 and around 35 Hz the coherence tends to 1. In particular, there is a peak which tends to 0.7 at around 10 Hz probably caused by nonlinear behaviour.

The tests are distinguished by increasing the excitation gain, while all other parameters are held constant to ensure controlled comparability. For the sake of completeness, the five measurements, along with corresponding setup parameters, are presented in the table below. The tests are distinguished by increasing the excitation gain, while all other parameters are held constant to ensure controlled comparability.

Test nr.	Excitation	Fs (Hz)	Gain (V)	fMin (Hz)	fMax (Hz)	Time length (s)
1°	Random	512	0.1	0	50	60
2°	Random	512	0.3	0	50	60
3°	Random	512	0.5	0	50	60
4°	Random	512	0.7	0	50	60
5°	Random	512	0.9	0	50	60

Table 4:List of the five measurements

The parameters are:

- **Type of Excitation**
  All measurements utilize random excitation, a broadband input signal that excites a wide range of frequencies simultaneously.
- **Sampling Frequency (Fs)**
  The sampling rate is consistently set at 512 Hz, which satisfies the Nyquist criterion for the specified frequency range (0–50 Hz).
- **Gain Variation**
  The gain, corresponding to the amplitude of the excitation signal applied to the shaker, is systematically increased from 0.1 V to 0.9 V in steps of 0.2 V.
  This allows for the investigation of nonlinear effects, such as amplitude-dependent shifts in resonance frequency, jump phenomena, or internal resonances that may emerge at higher excitation levels. The gain increment strategy is designed to progressively excite the system without introducing damage, starting from linear behavior (low amplitude) toward possible nonlinear responses at higher amplitudes.
- **Frequency Range and Duration**
  The excitation frequency band is kept constant between 0 Hz and 50 Hz, encompassing the expected fundamental and higher vibration modes of the structure. Each measurement has a duration of 60 seconds, which offers sufficient time to ensure statistical convergence of spectral estimates (e.g., Power Spectral Density, Frequency Response Function) while maintaining manageable data volumes.

Although the data obtained from the preliminary test are precise, they do not perfectly represent the actual dynamic behavior of the structure, as they are influenced by the measurement devices themselves. Specifically, the frame has an approximate mass of 21 grams, while the combined mass of the accelerometers, joined by a steel layer and two screws, which is about 15.3 grams. Having said that, it becomes necessary to analyze how much and how the weight of the assembled accelerometers influence the structural dynamics of the frame when it is subjected to the shaker vibration.
Furthermore, the presence of sensor cables affect the structural dynamic behavior. For what concerns the cables, it is crucial to consider their mass but also the damping effect. The damping effect refers to the phenomenon where vibrational energy is gradually dissipated in a mechanical system, typically resulting in a reduction in amplitude over time.
After taking into account the above considerations, three tests were performed:

- (i) with the accelerometers and cables installed on the structure
- (ii) with the accelerometers installed on the structure
- (iii) with bare frame only.

A major challenge in these tests lies in the data acquisition method. As solution, it is proceeding adopting a video-based methodology, wherein the response of the system is recorded according to three setups previously described. Subsequently analyzed using markers to track specific points.
The response signal was extracted using the Digital Image Correlation (DIC) technique. While the details of the DIC method are not the focus of this thesis, it was fundamental in capturing the structural response without introducing additional mass or damping through sensors or cables.
As anticipated, the results validated the initial hypothesis: the presence of the cables significantly influences the dynamic response of the system, notably affecting both the natural frequencies and the damping ratios. Finally, the same type of initial displacement was applied to the bare frame as in the accelerometer-only case, allowing for a comprehensive comparison of all three scenarios.
For each configuration (frame with accelerometers and cables, frame with accelerometers only, and frame only), the response data were processed to extract the natural frequencies and damping ratios. This analysis was conducted using the Linear Subspace Algorithm, which enables the estimation of modal parameters from measured time-domain data. The extracted values are summarized in the table below.

Configuration:	**1st Natural Frequencies**	**2nd Natural Frequencies**	**1st Damping ratio (%)**	**2nd Damping ratio (%)**
Accelerometers+Cables	9.6546 Hz	19.6754 Hz	0.4208	1.9861
Accelerometers-only	10 Hz	20 Hz	-	-
Frame-only	15.5 Hz	42.5 Hz	0.1416	0.1546

Table 5: list of modal parameters

For the case of accelerometers and cables, it has been used the NdB-method, which is a method widely adopted for extracting damping coefficients, to confirm the correct application of the algorithm cited before. The NdB method is based on the equation below and is applied just to the resonance zone of the response function. The two frequencies, Ω_A and Ω_B, are two points chosen because symmetric with respect to the axis passing through the natural frequency and distant n decibels from the peak in correspondence of the natural frequency.

$$\zeta = \frac{1}{\sqrt{n-1}} * \frac{\Omega_A - \Omega_B}{2\omega_n}$$

The procedure has been repeated twice for the two natural frequencies, taking two different n in order to have the two frequencies points as close as possible to be symmetric to the axis. From the first frequency, the one corresponding to the horizontal resonance of the system, to the second natural frequency, the one corresponding to the vertical resonance, are graphically showed in the pictures below, highlighting the chosen points.
In conclusion, the parameter extraction has been conducted adopting the test portrayed with the lowest amplitude since it represents the case where the nonlinearities have the lowest effect.

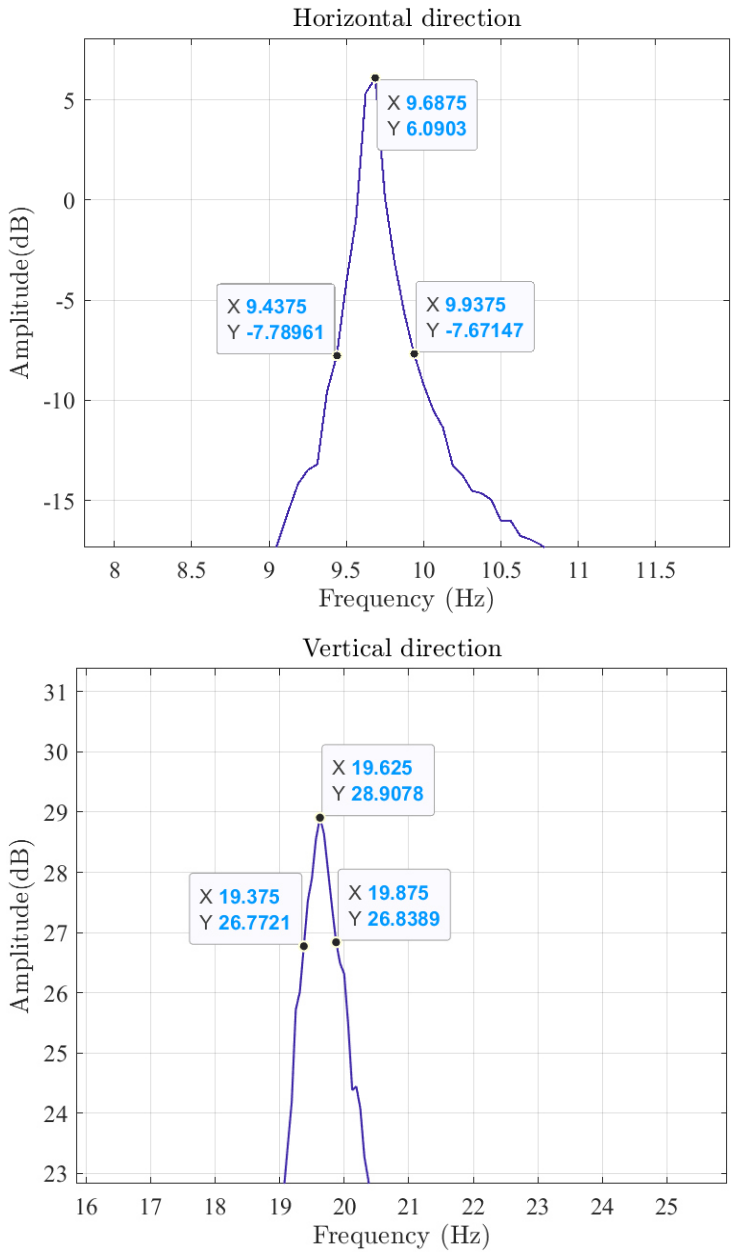

Figure 3.2.6: two images of the resonance peaks. It is identified also the points to which the NdB method is applied.

3.3 Model updating

The model updating approaches that will be used in this research are::

- Solidworks model: a model built on the Solidworks platform on which is possible performing analysis, such as modal analysis, in order to compare the obtained data with the experimental data.
- Linear Ansys APDL: a model built on the Ansys APDL allow to obtain more accurate data which will be compared to the experimental results.
- Nonlinear Ansys APDL: a model built on Ansys APDL using nonlinear elements.

Solidworks model

Once the results of the analytical model and of the experimental tests show agreement, a model is designed on two different software, SolidWorks and Ansys, where nonlinear analysis are conducted.

Initially, the model is designed on SolidWorks: the software permits to compute easily the modal analysis so it offers a valid alternative to Ansys, the software which will be adopted in modal analysis and in transient analysis.
Firstly, the frame only is analysed, then the frame with accelerometers. The sizes of the frame are the ones retrieved through iterations. The table below shows the data which are compared to the experimental measurements.

	Solidworks		**Experimental measurements**	
Frame-only	15.57 Hz	44.99 Hz	15.70 Hz	42.70 Hz
Frame with accelerometers	9.95 Hz	19.65 Hz	9.7 Hz	19.7 Hz

Table 6: List of natural frequencies obtained by Solidworks and by experimental measurements

Ansys APDL model

Then, the same type of study is conducted on Ansys APDL. The software Ansys APDL is quite different from Solidworks; Ansys APDL is meant for structural analysis. In this chapter it is done the modal analysis to catch the vibration characteristics of a structure. The first step toward the simulation is the definition of the model, keeping in mind that only linear behaviour is valid in a modal analysis and material properties can be linear, isotropic or orthotropic, and constant or temperature-dependent.

Eventually, the constraints are defined which are simply the two points connected to the shaker and then the simulation can be done. The analysis is portrayed with models built with different number of elements.

	Ansys Apdl		**Experimental measurements**	
Frame-only	15.441 Hz	44.775 Hz	15.70 Hz	42.70 Hz
Frame with accelerometers	9.97 Hz	19.92 Hz	9.7 Hz	19.7 Hz

Table 7: List of natural frequencies obtained by Ansys APDL and by experimental measurements

Nonlinear ANSYS model

The preliminary study, the modal analysis, is the basis for the transient dynamic analysis.

The transient dynamic analysis is a technique used to determine the dynamic response of a structure under the action of any general time-dependent loads. The transient dynamic analysis requires more computer resources so it is important to reduce the number of elements. The simulation is portrayed according to three different models, each of which has a different number of elements. Nonlinear structural behaviour arises from a number of causes, which can be grouped into these principal categories: changing status, geometric nonlinearities, material nonlinearities.

In this case, the nonlinear geometries are considered. If a structure experiences large deformations, its changing geometric configuration can cause the structure to respond nonlinearly.

Firstly, the model used for the transient dynamic analysis a the simplest one, meaning that is the one with the lowest number of elements. The model is the one used for the modal analysis.

Secondly, after the definition of the model, it is necessary to establish the initial conditions, the conditions at time 0, and then apply the loads which are functions of time. The initial conditions for such calculations are:

- Initial displacement equal to 0,
- Initial velocity equal to 0,
  Initial acceleration equal to 0.

Then it is possible to define the load varying time characteristics:

- The type of load is the vertical displacement
- It is applied to the base of the portal frame
- It is a sine wave, starting and ending with a transitory phase

For the transient dynamic analysis, it has been chosen a duration of 10 seconds and an amplitude of 1 millimetre. Such parameters could change in other simulations. The analysis is portrayed on ANSYS APDL, adopting a model with 32 elements. It is necessary to establish also the sampling frequency of the input, the base displacement, and of the output, the displacement of some nodes of the portal frame. Hence, the structure is subjected to a sine wave oscillation applied to the nodes located at the base and it is studied the response to such inputs.

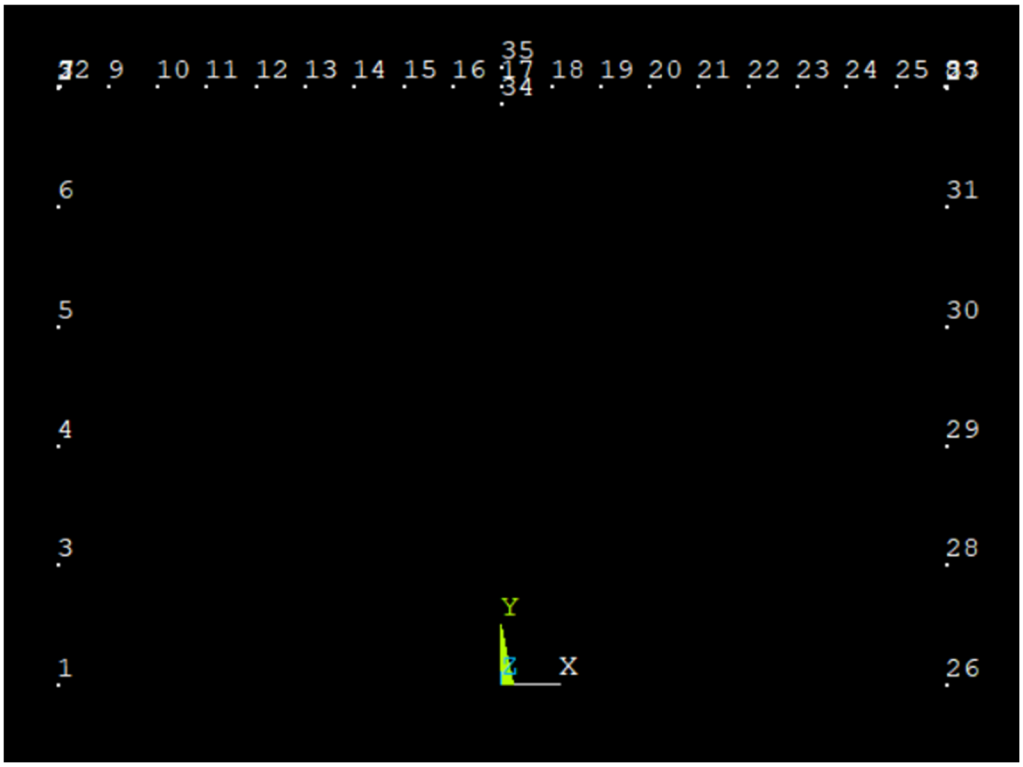

Figure 3.3.1: Geometry of the frame with numbered nodes (32 elements)

The following results shows what it has been looking for in this thesis: the internal resonance. It is clearly visible in the picture: the portal frame subjected to vertical displacement starts to vibrate horizontally where at approximately 5 seconds the amplitude of oscillation increase. The legend in the picture represents at which nodes correspond the line while, using the picture above, it is possible to understand which is the node.

For what concerns the power spectrum density, which is a measure that describes how the power of a signal, it is distributed across different frequencies, the picture shows several peaks but with low decibels. Even if the value of the peaks is low, it is assumed that is present harmonic distortion.

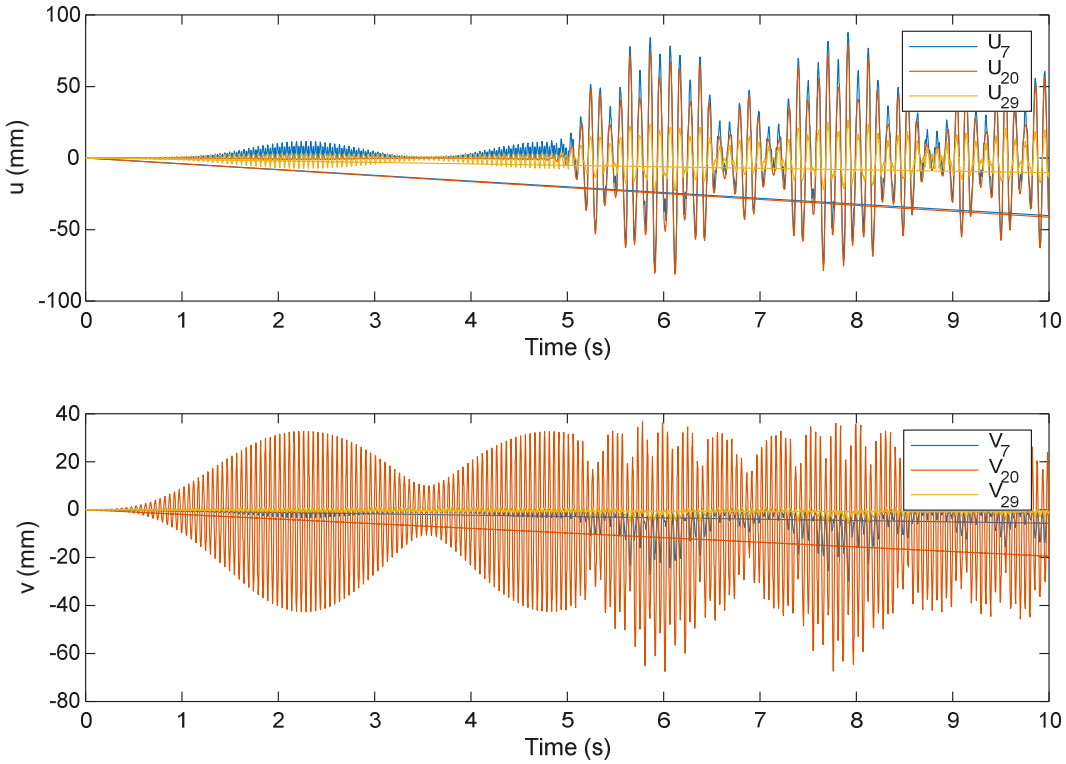

Figure 3.3.2: Displacements along x (u) and along y (v) directions

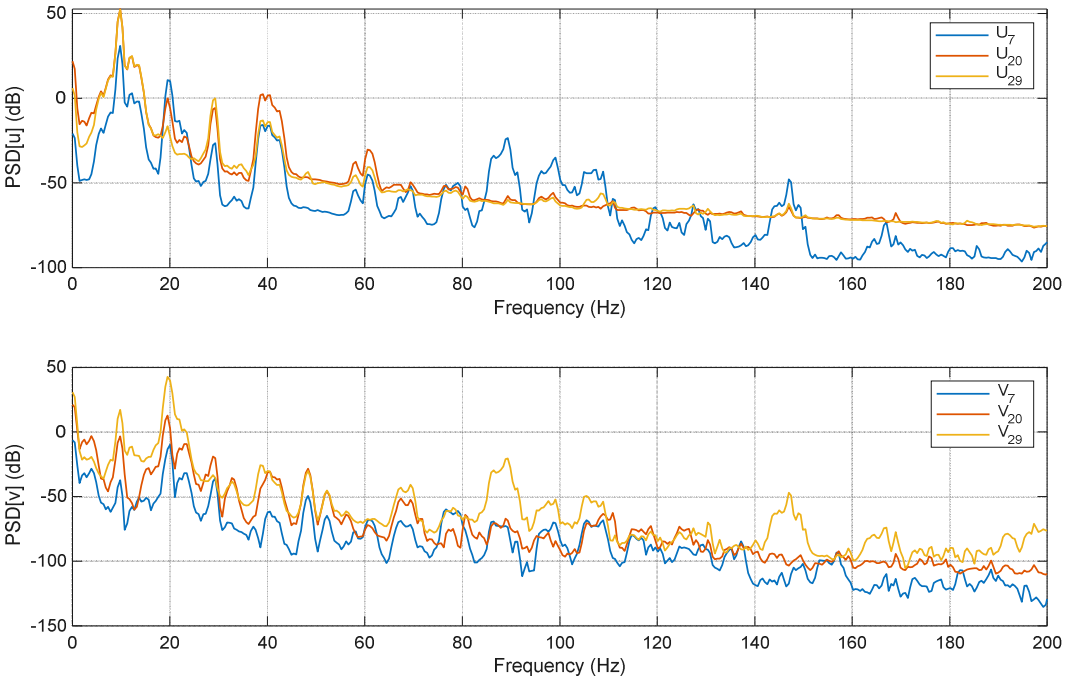

Figure 3.3.3: PSDs of both signals: u and v

The internal resonance is clearly visible also through an animation of the system. Three images at different instant of time are displayed below

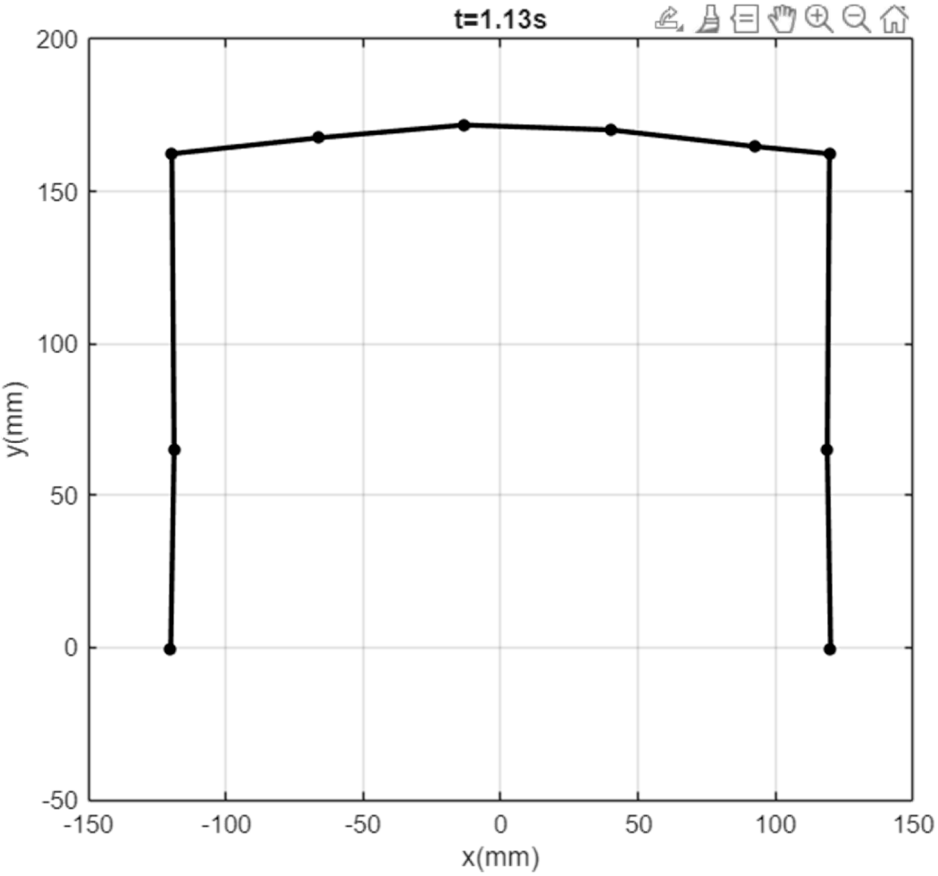

Figure 3.3.4: First sketch of the animation

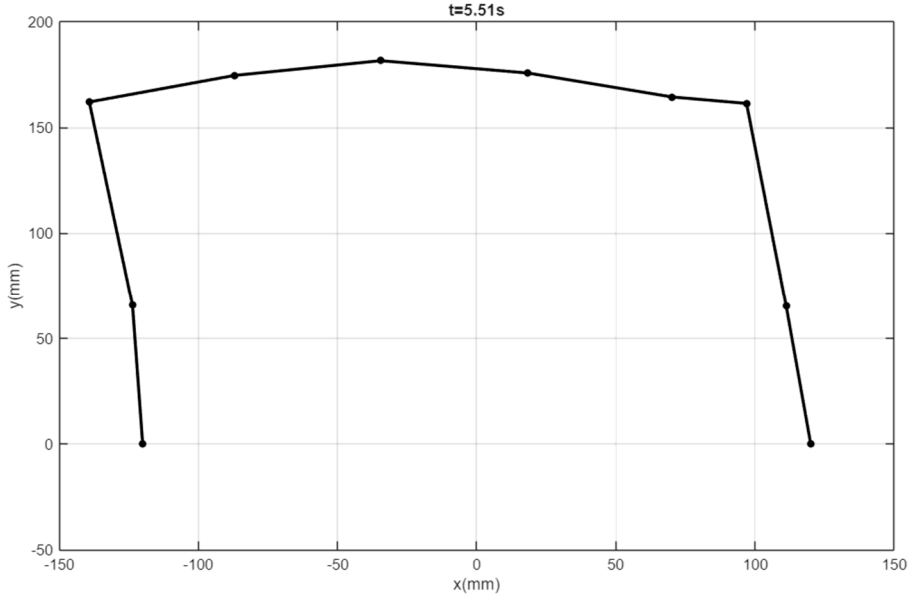

Figure 3.3.5: Second sketch of the animation

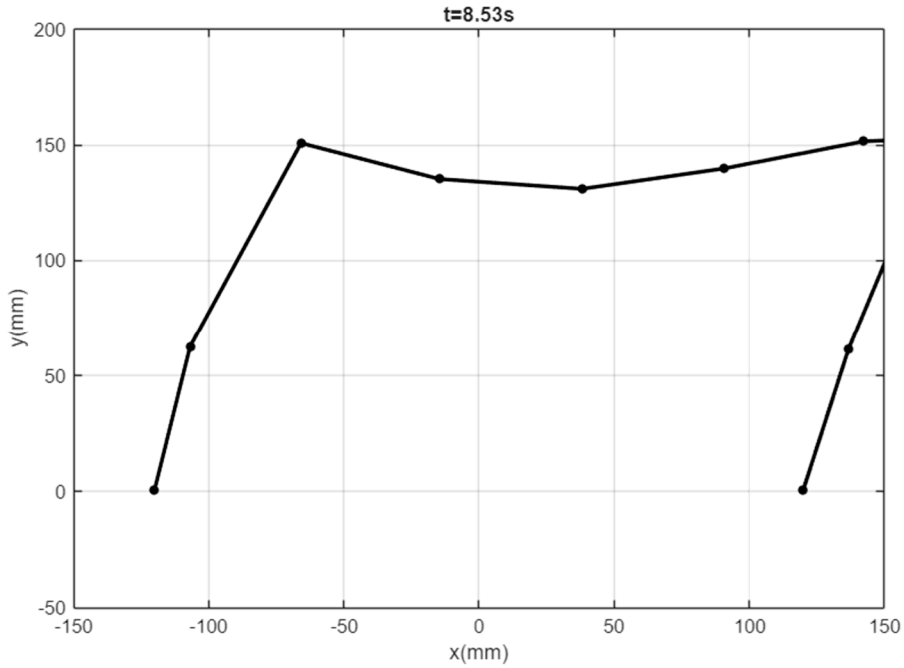

Figure 3.3.6: Third sketch of the animation

Although internal resonance is observed in one measurement, it is not evident in the others. For instance, the images below correspond to a different measurement, which differs from the previous one only in terms of the time interval and of the number of elements. In this case, the vertical displacement does not influence the horizontal response, indicating the absence of internal resonance. Furthermore, the power spectral density exhibits peaks solely at the system's natural frequency, supporting this observation.

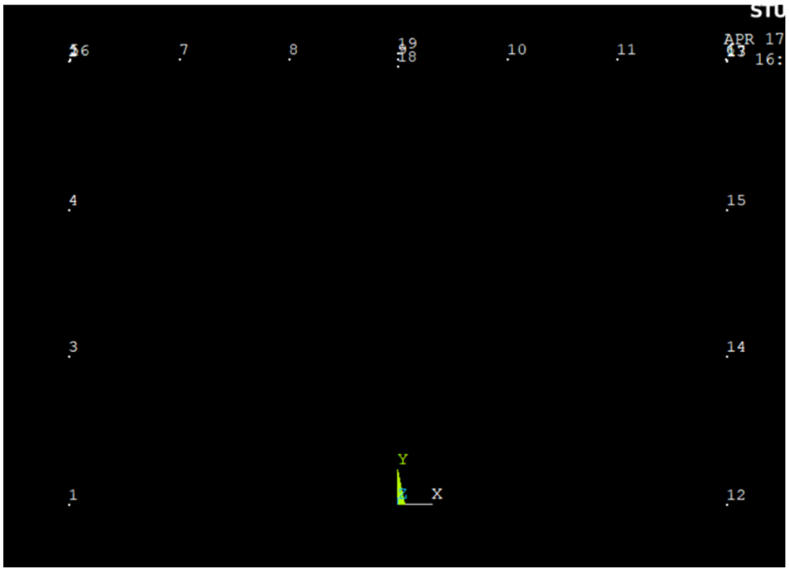

Figure 3.3.7: Geometry of the frame with numbered nodes (16 elements)

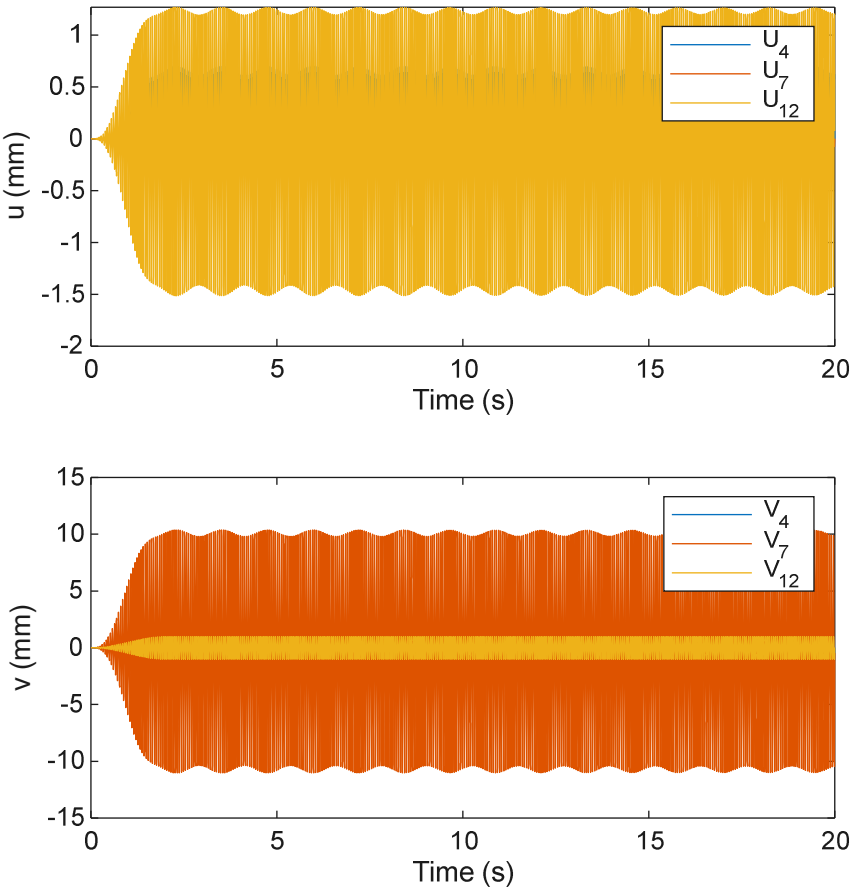

Figure 3.3.8: Displacements along x (u) and along y (v) directions

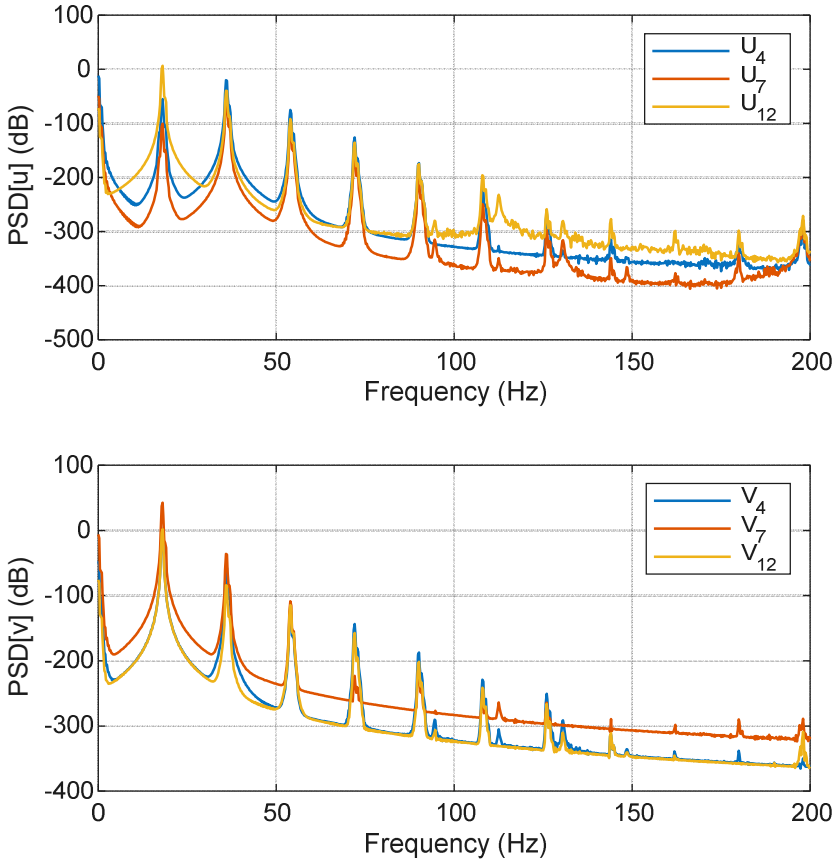

Figure 3.3.9: PSDs of both signals u and v

Evaluation of the measured data

The data obtained from both SolidWorks and ANSYS APDL simulations are presented below. A significant discrepancy is observed when the portal frame is not instrumented with accelerometers, whereas the results for the frame equipped with accelerometers align more closely with the experimental measurements. This variation is anticipated, as data acquired through Digital Image Correlation (DIC) methods tend to be less accurate than those obtained via accelerometers. Consequently, greater emphasis is placed on minimizing discrepancies in the configuration involving accelerometers, as it provides a more reliable basis for comparison with experimental data.

	Ansys Apdl		**Solidworks**		**Experimental measurements**	
Frame-only	15.441 Hz	44.775 Hz	15.57 Hz	44.99 Hz	15.70 Hz	42.70 Hz
Frame with accelerometers	9.97 Hz	19.92 Hz	9.95 Hz	19.65 Hz	9.7 Hz	19.7 Hz

Table 8: Complete list of natural frequencies from ANSYS APDL, Solidworks and Experimental measurements

4. Experimental verification with piezoelectric VEH

The mechanical system has been subjected to:

- Run up and down at a frequency of 19 Hz
- Random vibrations
- Random vibrations using piezoelectric devices

The experimental setup is shown below: it is used only one piezoelectric device and is installed in the lower part of the frame.

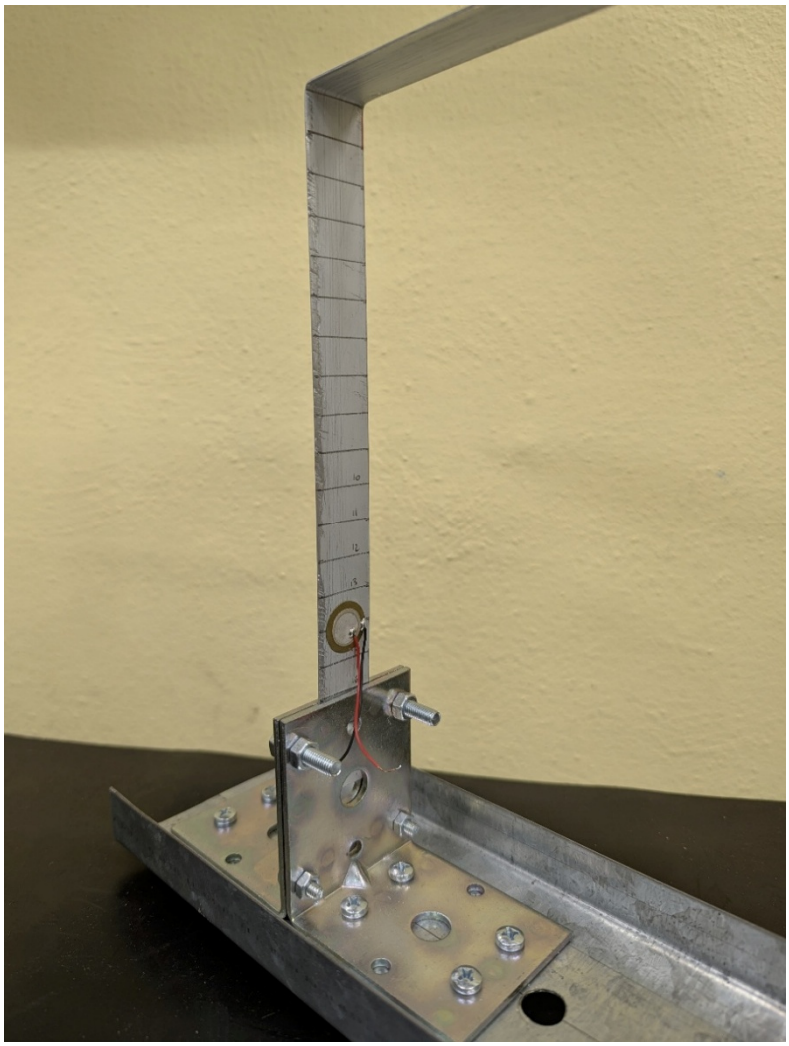

Figure 7.1: Picture of the piezoelectric device installed on the portal frame

It is also possible to visualize how the setup is done in the picture below.

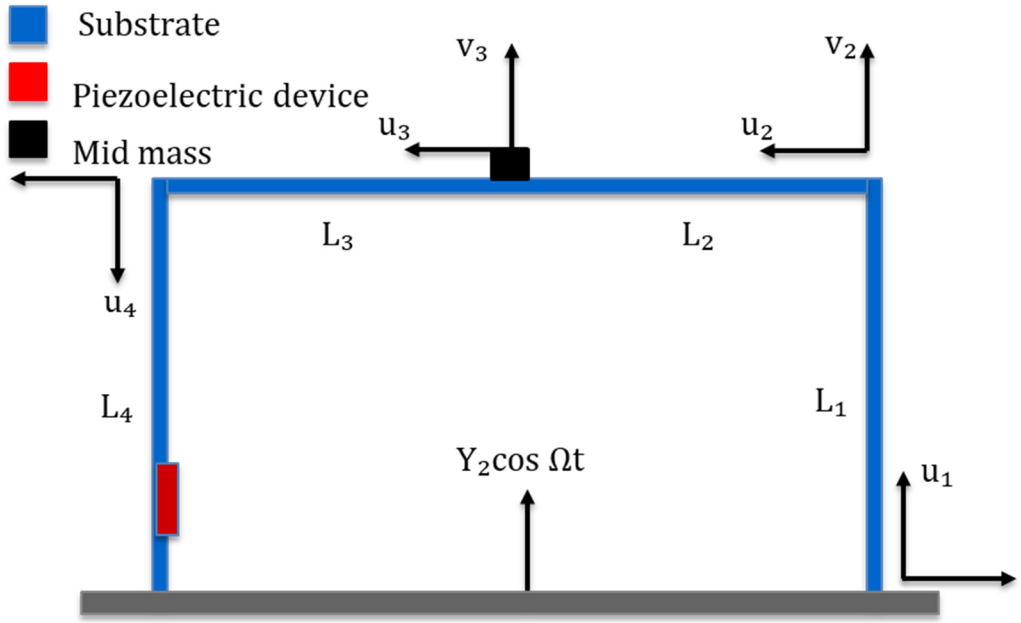

Figure 4.2: Diagram of the portal frame with mid mass and piezoelectric device

From the mechanical model, object of the research, the measured data are:

Random vibrations

The portal frame is subject to two types of random vibrations: the first random vibration is characterized by low amplitude while the second is characterized by high amplitude of oscillations.

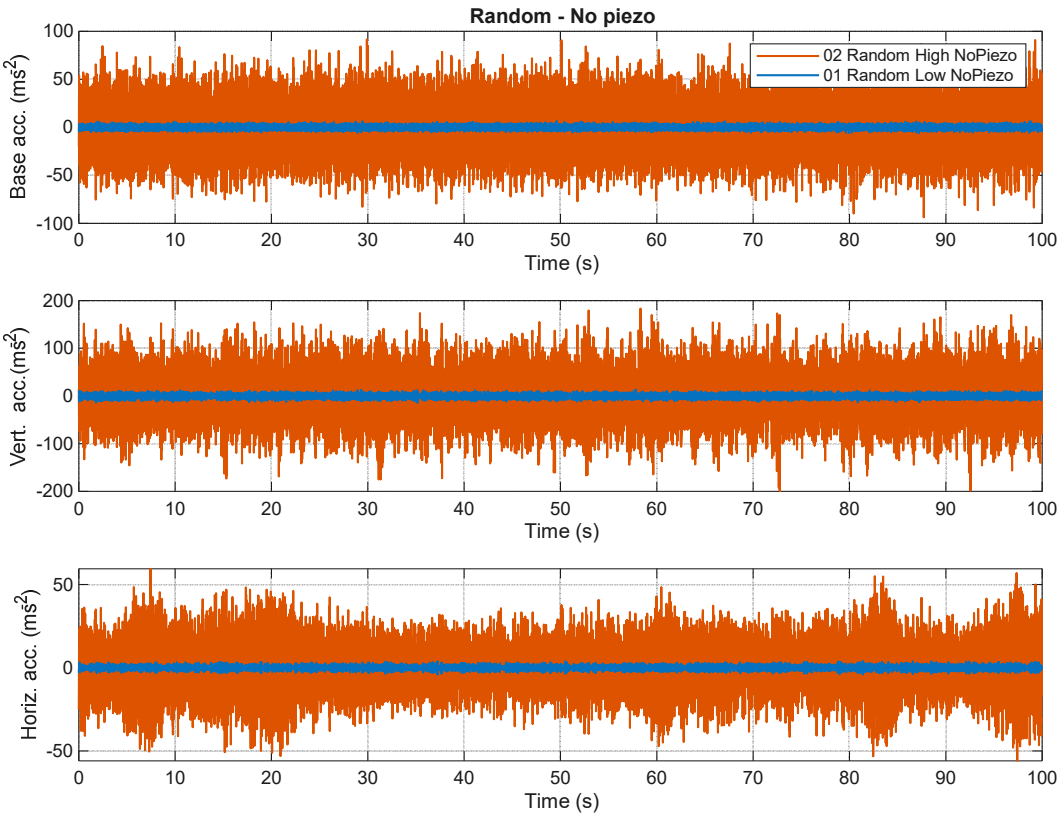

Figure 4.3: Diagrams of the base acceleration, of the relative vertical acceleration and of the horizontal acceleration

Moreover, the power spectrum densities of the signals are studied. The peaks of the two signals are not coincident because of the effect of nonlinearities, indeed, as already explained, large amplitude of oscillation is responsible for the incurrence of nonlinear behaviour.

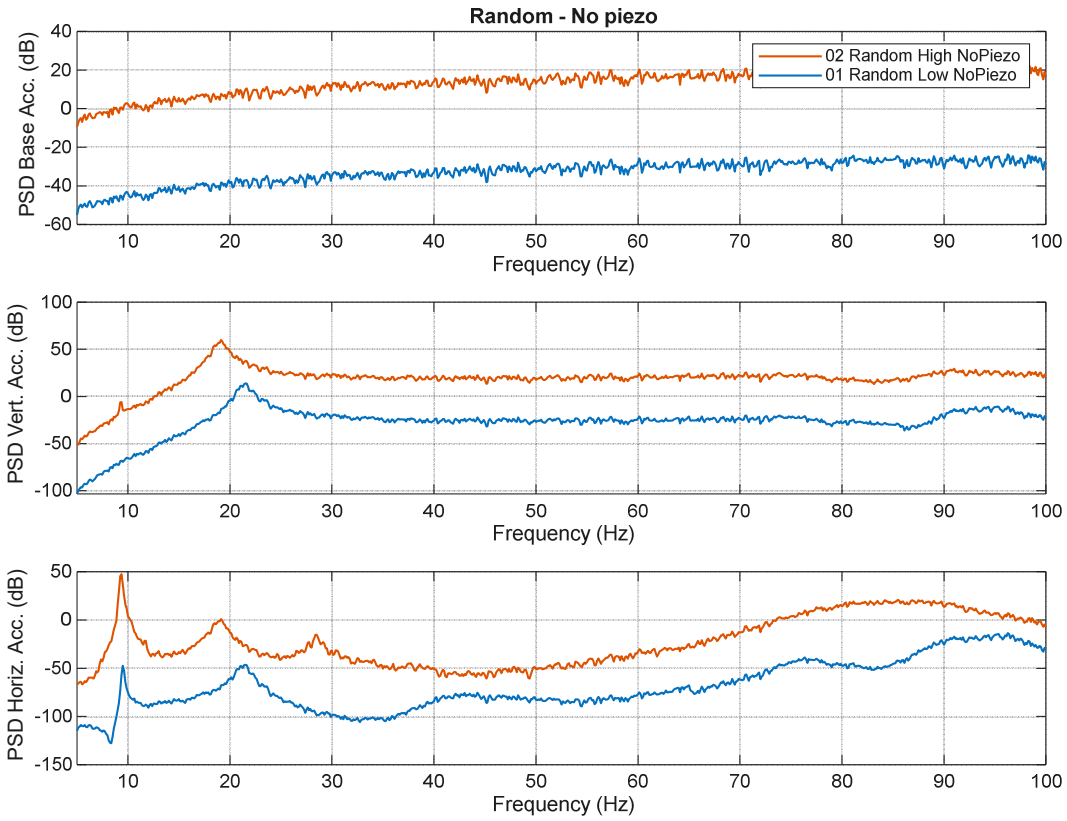

Figure 4.4: Diagrams of the PSDs of the base acceleration, of the vertical acceleration and of the horizontal acceleration.

For what concern the transmissibility, the following picture shows vertical and horizontal acceleration transmissibility for the two excitation levels.

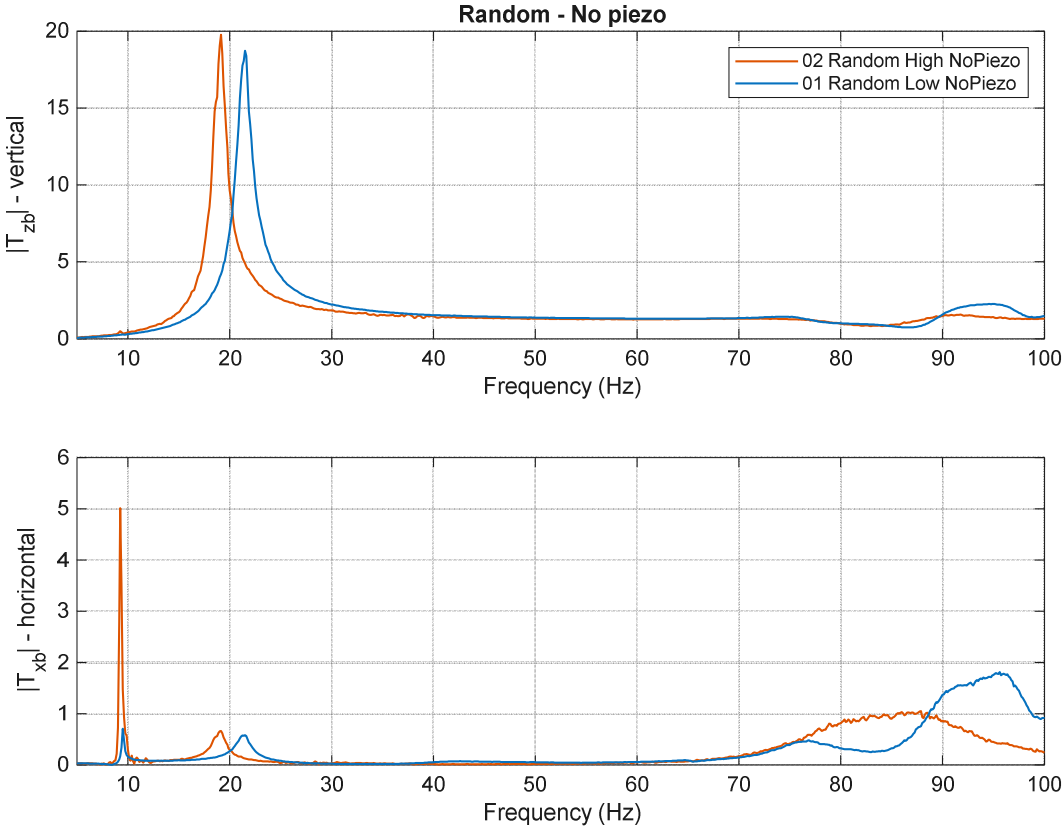

Figure 4.5: Diagrams of the vertical and horizontal transmissibility

Random vibrations using piezoelectric devices

The following image describes the base acceleration, the vertical acceleration and the horizontal acceleration with a high gain of measurement, a high amplitude of oscillation.

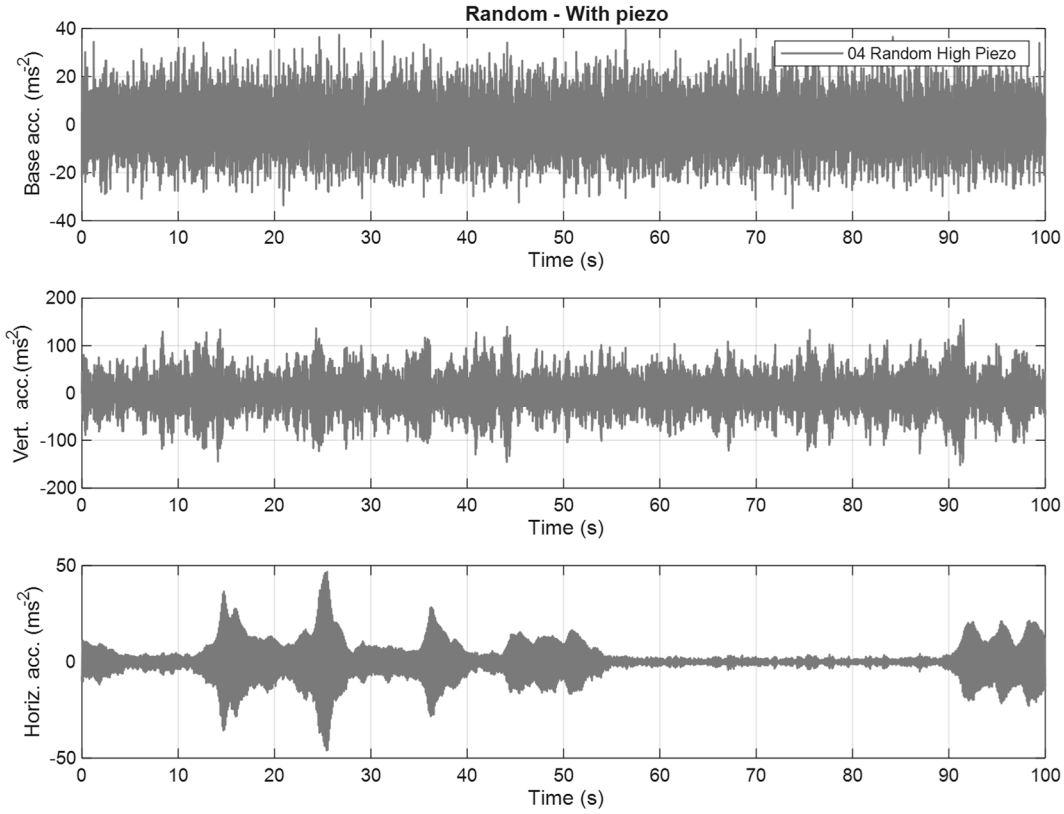

Figure 4.6: Diagrams of the base acceleration, of the relative vertical acceleration and of the horizontal acceleration

Unlike the previous case, in the next image it is present also the voltage function, thanks to the presence of piezoelectric devices. The voltage has two peaks corresponding to the two natural frequencies.

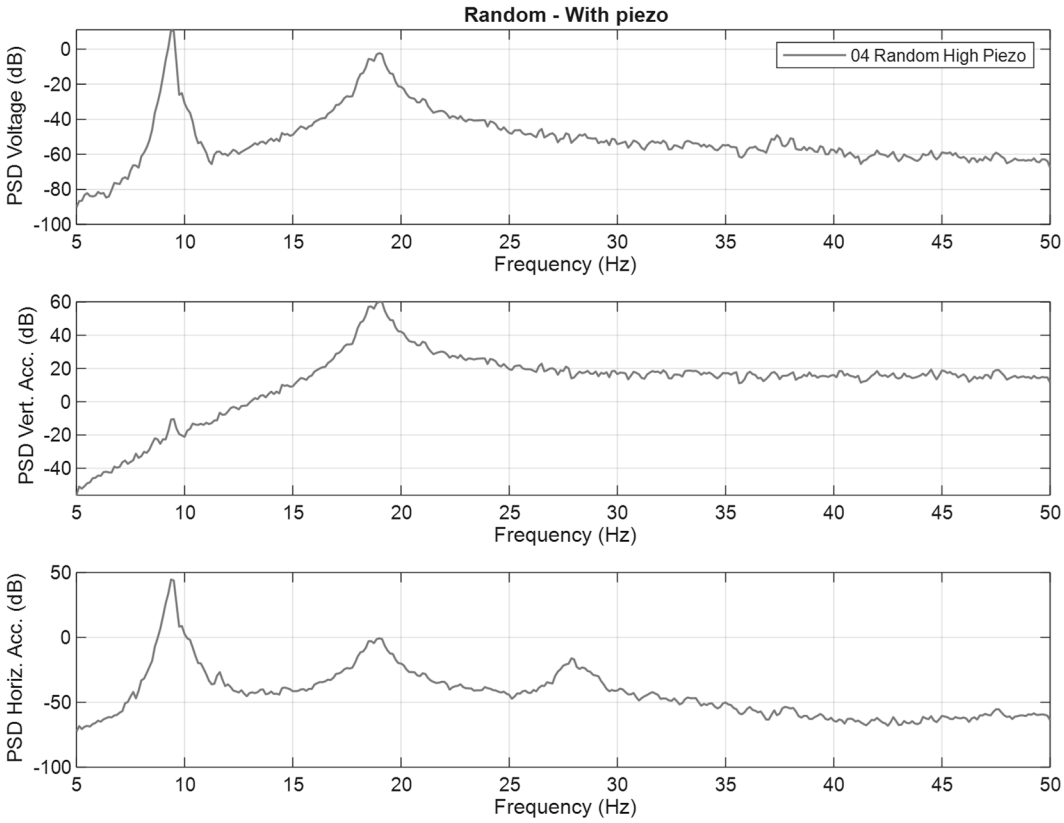

Figure 4.7: Diagrams of the PSDs of the voltage signal, of the vertical acceleration and of the horizontal acceleration.

Finally, both vertical and horizontal transmissibility are plotted in the graph below.

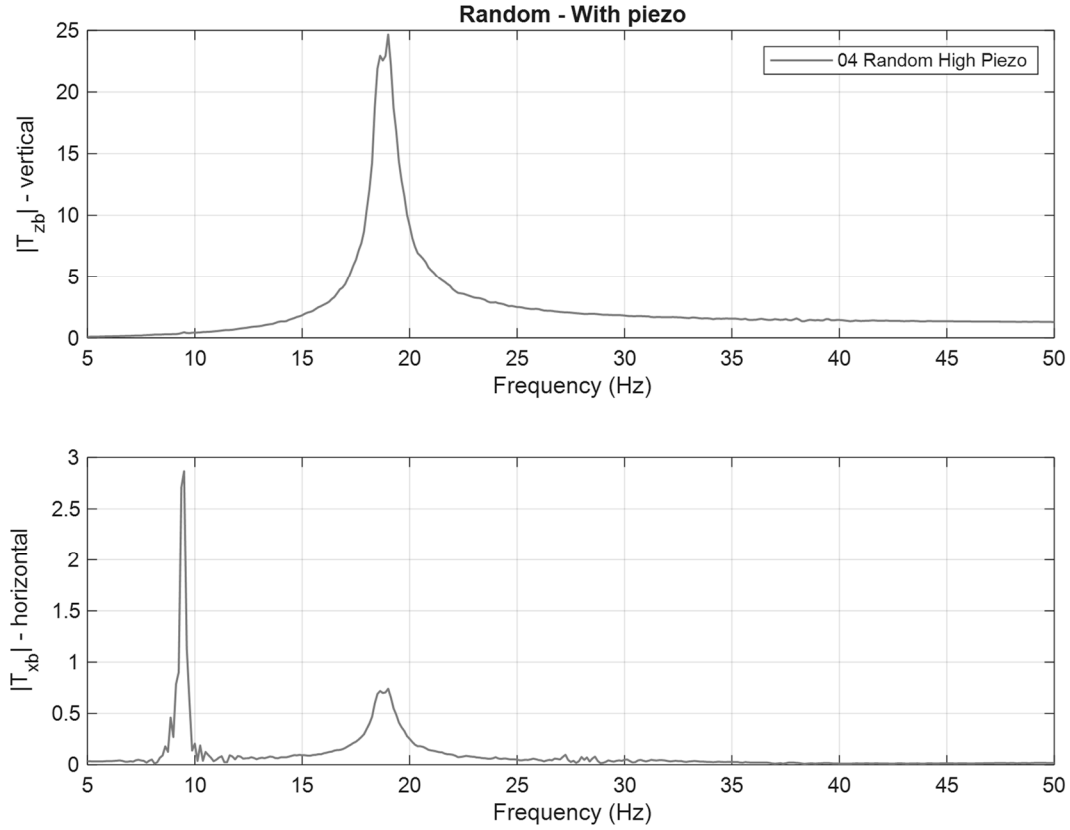

Figure 4.8 Diagrams of the vertical and horizontal transmissibility.

Run up and down of sine at frequency 19 Hz

The portal frame is subjected to a base acceleration of 2 m/s^2 and the output of piezoelectric system is analysed.

The first picture shows two graphs: the first represent the base acceleration while the second represent the acceleration of the accelerometer positioned at the middle of the horizontal beam. The first graph doesn't need to focus on, it simply represent the base acceleration. The second graph is noteworthy since it is evident the presence of the internal resonance. In the color blu is visible the vertical motion of the accelerometer while in the color orange the horizontal motion. When the frame starts to oscillate horizontally, the oscillations of the orange line starts to increase, there is visible the internal resonance.

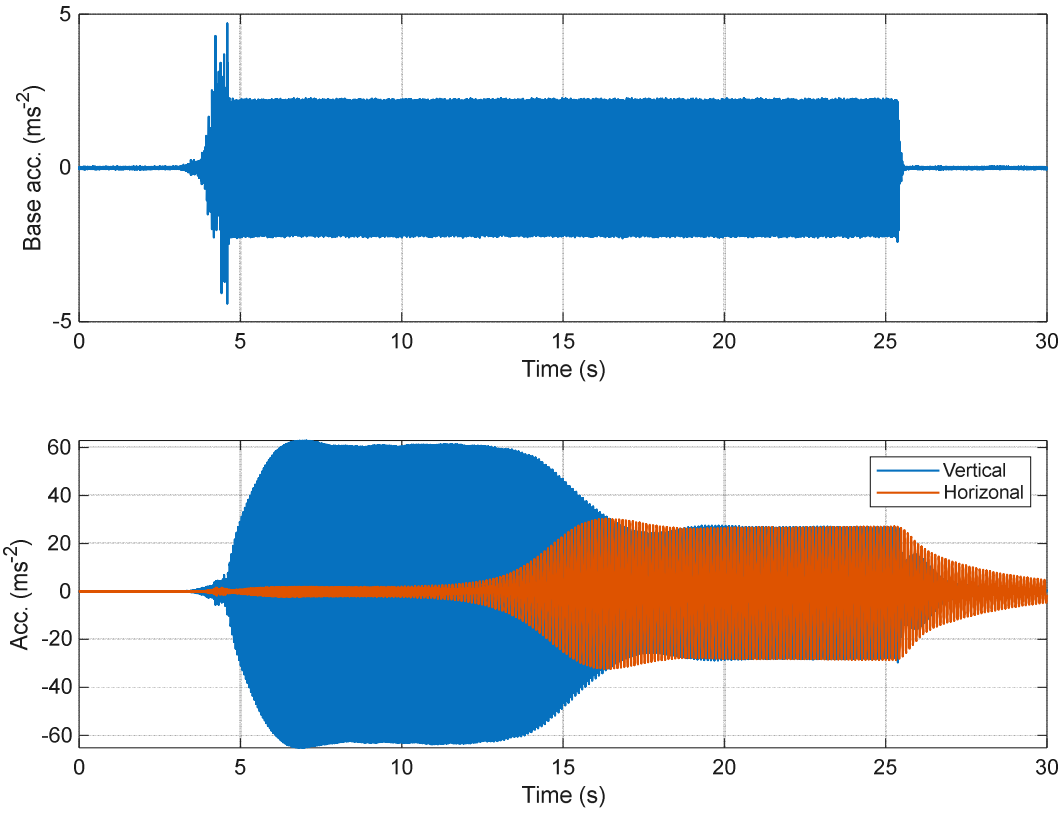

Figure 4.9: Diagrams of the base acceleration and of both vertical and horizontal accelerations.

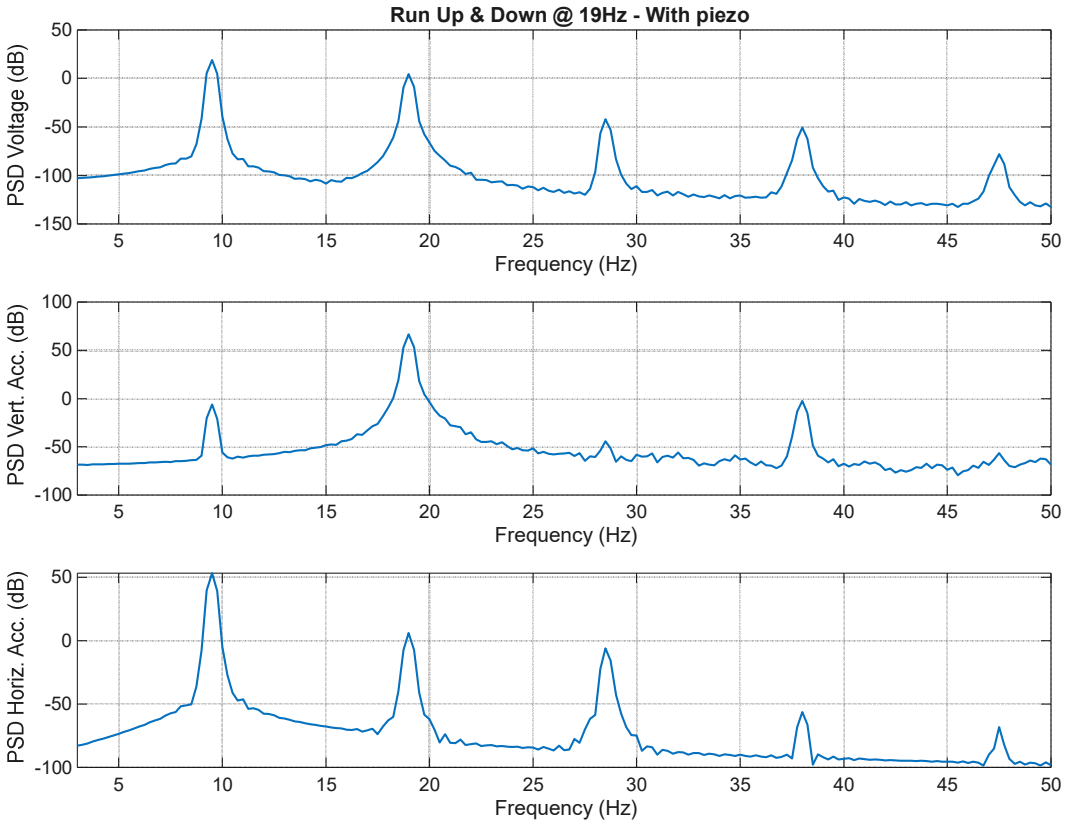

Figure 4.10: Diagrams of the PSDs of the voltage, of the vertical acceleration and of the horizontal acceleration

A spectrogram is a visual representation of the frequency spectrum of a signal as it varies over time. It shows how the energy or intensity of different frequencies changes across time. The spectrograms characteristics:

- The horizontal axis (x-axis) represents time.
- The vertical axis (y-axis) represents frequency.
- The colour or brightness of each point indicates the amplitude (intensity) of a particular frequency at a particular time

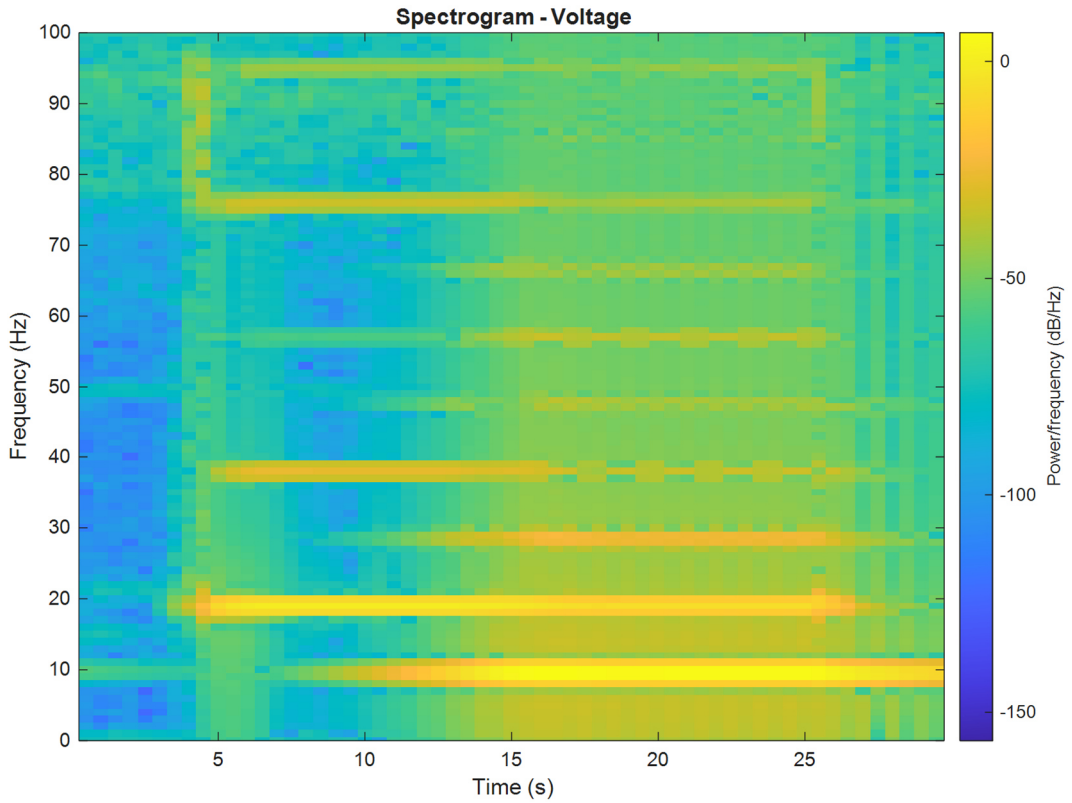

Figure 4.11: Spectogram

5. Conclusions and Future Work

1. Summary and Objectives

This research was undertaken to investigate the dynamic behavior of a vibration energy harvester (VEH) exhibiting nonlinear internal resonance and utilizing piezoelectric materials for energy conversion. The study aimed to develop a reliable digital twin of the VEH system, combining both linear and nonlinear modeling approaches, and to validate these models through experimental measurements. Particular attention was given to the influence of measurement instrumentation, especially the impact of accelerometers and their associated cabling, on the modal properties of the structure.

The scope of this work included the design and modeling of the VEH using SolidWorks and ANSYS APDL, the performance of preliminary modal and transient analyses, and the execution of experimental campaigns incorporating both traditional accelerometer-based measurements and non-contact Digital Image Correlation (DIC) techniques.

2. Main Findings

2.1 Internal Resonance and Nonlinear Dynamics

The study confirmed the presence of internal resonance within the VEH structure, specifically a 2:1 modal interaction that broadens the system's effective frequency response. This phenomenon was both predicted by nonlinear simulations and observed experimentally, particularly under sinusoidal base excitation near 19 Hz. The nonlinear coupling between vibration modes enhances energy harvesting performance by increasing the bandwidth over which significant power can be extracted.

2.2 Influence of Accelerometers and Cabling

Experimental and numerical analyses demonstrated that the mass of the accelerometers significantly affects the dynamic behavior of the structure. Specifically, their addition leads to a measurable reduction in the system's natural frequencies. While this mass effect is easily derivable, the influence of the connecting cables proved more complex. The cables contribute not only to additional mass but also to increased damping, altering both frequency and energy dissipation characteristics of the frame. Although simplifications were employed (e.g., modeling cables as lumped masses), these do not fully capture the distributed and frequency-dependent nature of the cable dynamics.

2.3 Experimental Techniques and Data Analysis

The combined use of accelerometers and DIC enabled a comprehensive assessment of VEH's response. Accelerometers offered precise point measurements of modal frequencies and damping ratios, while the DIC system provided displacement data, enabling mode shape visualization. Data analysis was performed using linear subspace identification algorithms, and damping estimates were further validated using the -NdB method.

3. Reflections on Modeling and Methodology

The use of finite element models in both SolidWorks and ANSYS APDL was instrumental in developing a digital twin of the VEH system. Modal analysis in SolidWorks provided a rapid design-validation loop, while ANSYS APDL enabled more advanced nonlinear transient simulations. Such simulations were crucial for predicting the onset and evolution of internal resonance phenomena.

Nonetheless, the modeling assumptions, particularly the exclusion of cable flexibility and damping, as well as the reliance on linear piezoelectric material models—were needed. While the match between simulations and experiments was acceptable within the primary frequency range, discrepancies emerged at higher frequencies and amplitudes.

4. Limits

Several limits emerged during the research:

- The complex influence of measurement cables was not fully captured by the numerical model. Despite iterative mass adjustment strategies, the actual damping and inertial effects of cables remain only partially understood.
- Internal resonance is a dynamic phenomenon that remains at the forefront of current research. Due to its nonlinear and complex nature—characterized by modal energy transfer, frequency coupling, and amplitude-dependent behavior—accurately capturing it in numerical simulations poses significant challenges. Commercial finite element software such as ANSYS APDL, while highly effective for linear and or mildly nonlinear problems, struggles to fully reproduce the intricate dynamics of internal resonance. Such limitations arise from the difficulty in modeling strong mode interactions and geometric nonlinearities.
- The experimental setup constrained excitation to a fixed direction (vertical), limiting exploration of multi-directional input cases.

5. Future Work

The findings of this thesis suggest several directions for future investigation:

- **Advanced Cable Modeling:** Incorporating flexible-body dynamics or distributed parameter models to more accurately represent cabling effects.
- **Wireless Sensing:** Exploring the use of lightweight or wireless accelerometers to reduce mass-loading effects.
- **Control and Adaptivity:** Investigating active or passive control strategies that exploit internal resonance to optimize harvesting under varying excitation conditions.
- **Material Modeling Enhancements:** Including nonlinear or hysteretic piezoelectric material models to better predict electromechanical coupling behavior at higher excitation levels.
- **Software limit:** Future work could focus on developing hybrid modeling frameworks that couple finite element simulations with reduced-order models (ROMs) or machine learning-based surrogate models. These approaches could allow more efficient and accurate prediction of complex nonlinear behaviors like internal resonance. Additionally, implementing user-defined elements or integrating ANSYS APDL with external solvers (e.g., MATLAB, Python-based nonlinear dynamic libraries) may offer greater flexibility for capturing modal interactions. Experimental validation under varying excitation profiles, multi-directional inputs, or under operational loads would further support the reliability of these models and extend their applicability to real-world energy harvesting systems and structural health monitoring platforms.

6. Concluding Remarks

This study has demonstrated that internal resonance mechanisms in VEH systems can be harnessed to improve performance over a broader frequency spectrum. Through the integration of analytical, numerical, and experimental techniques, a validated digital twin of the system was developed. The impact of instrumentation, particularly sensor mass and cable dynamics, was systematically evaluated, highlighting the need for careful experimental design and model calibration.

The results provide a robust foundation for future research in nonlinear energy harvesting systems and digital twin development for adaptive and resilient energy solutions.

References

[1] P. F. P. Ali H. Nayfeh, Linear and Nonlinear Structural Mechanics, Wiley, 2004.

[2] L.-Q. C. Hu Ding, «Li-Qun Chen,» *Nonlinear Dynamics,* p. 47, 2020.

[3] Y. F. Li-Qun Chen, «Internal resonance vibration-based energy harvesting,» *Springer Nature,* p. 25, 2023.